Doctoral Dissertation

Rapid adaptation to spatial goals through activation of the ventral tegmental area-hippocampal dopaminergic pathway

Yuta Tamatsu

Graduate School of Brain Science, Doshisha University

A thesis submitted for the degree of

Doctor of Philosophy in Science

Mar. 2024

Abstract

This study explores how dopamine regulates the adaptive behavior of animals in pursuing rewards in response to environmental changes. Specifically, it investigates whether the action of dopamine within the hippocampus is crucial in memory and adaptation to spatial tasks.

At the heart of this research is the dopaminergic pathway from the ventral tegmental area (VTA) to the hippocampus. We examined how this pathway is involved in the persistence and adaptation of spatial goals. Specifically, we observed the behavior of mice with dopaminergic neuron lesions in the VTA in a circular maze where reward locations frequently changed.

The results showed that mice with damage to VTA dopaminergic neurons struggled to learn and update the locations of rewards. This suggests that VTA dopaminergic neurons play a significant role in the persistence and adaptation of spatial memory. Moreover, these mice exhibited symptoms of motor impairment and loss of motivation, even when dopamine receptors in the dorsal hippocampus were selectively blocked.

Further, stimulating VTA dopaminergic axons within the dorsal hippocampus improved the mice's ability to adapt to changing reward locations. These findings indicate that the

dopaminergic pathway within the hippocampus plays an important role in adaptation to spatial goals.

Overall, this study provides new insights into the role of dopamine in the hippocampus and how it affects the process of animals persisting with and adapting to spatial goals in new environments.

Acknowledgment

I would like to express my deepest gratitude to my supervisor, Dr. Susumu Takahashi, for his continuous guidance, scientific advice, and encouragement during the last five years. This doctoral thesis is largely based on the research presented in my published papers (Tamatsu et al. 2023), a testament to the invaluable insights and data gathered through these works. I also thank Dr. Hirotsugu Azechi, Dr. Ide Kaoru, and the past and present lab members for their encouragement and insightful comments on this research. I want to give special thanks to members of my thesis committee, Dr. Jun Motoyama, Dr. Yoshito Masamizu, and Dr. Takeshi Sakaba, for their time and efforts in my examination. I am also grateful to the Japan Science and Technology Agency (JST) SPRING and Doshisha University for their financial support. Finally, I wish to extend my sincere gratitude to my family for their understanding, support, and encouragement. I would not have been able to complete this study without their dedication.

Table of contents

List of Figures and Table

Figures

Table

Chapter 1. Introduction

1.1 Goal-directed Spatial Navigation

Goal-directed spatial navigation is a fundamental behavioral ability in animals to efficiently search for essential resources such as food, nests, and mates. This behavior has an ecological and evolutionary background and has developed as one of the survival tactics of animals. Animals continuously gather abundant sensory information from their environment. They use cues from not only vision and olfaction but also hearing, touch, and even magnetoreception to identify changes in the environment and the location of goals (Jain, Jakhalekar, and Deshmukh 2017; Naisbett-Jones and Lohmann 2022; Yamada et al. 2020). This sensory information is extremely important when animals formulate safe and effective movement routes. In formulating these movement routes, sensory information is not the only factor; understanding and recalling routes to specific destinations, that is, learning and memory of routes, are also crucial. Learning and memory are particularly important as long-term survival strategies. For example, animals learn spatial information about locations where food becomes abundant in certain seasons, the whereabouts of water sources, or areas inhabited by predators, and they formulate their movement routes based on these memories. At the heart of this process of spatial learning and memory is the hippocampus in the brain, which plays a central role (J.

Lisman et al. 2017). The hippocampus regulates the process of learning and memory through synaptic plasticity formed based on experiences. Previous research has found pyramidal cells in the hippocampus, known as place cells, which code for information about one's current location (O'Keefe and Dostrovsky 1971; Tolman 1948). Recent studies have also discovered cells in the hippocampus that fire around the location of rewards (Gauthier and Tank 2018). These cells are called reward cells. Unlike place cells, reward cells code for the location of rewards. Furthermore, while place cells change their activity patterns when the external environment changes, reward cells do not have this property, and a specific group of cells consistently fires around the location of rewards.

From the above, it can be considered that there is a deep relationship between the hippocampus and rewards in goal-directed spatial navigation behavior.

1.2 Reward and Dopamine

Reward refers to the benefits or gains acquired because of specific actions or choices, and it functions as an important factor in enhancing motivation and promoting behavior. In a biological context, animals choose and adjust their behavior according to the environment, receiving rewards or penalties as a result. This environmentally adapted behavior selection is based on a learning mechanism known as reinforcement learning, with reward prediction error acting as its core. Specifically, reward prediction error represents the difference between the predicted reward and the actual reward received (Schultz, Dayan, and Montague 1997), and this discrepancy plays a crucial role in the processes of learning and decision-making (Lerner, Holloway, and Seiler 2021). The basal ganglia are deeply involved in these processes of learning and decision-making. The basal ganglia play various roles in motor control, recognition of rewards, learning, and decision-making. For instance, in motor control, they optimize fine movements and bodily movements, and abnormalities in them can lead to neurological disorders such as Parkinson's disease. In learning and decision-making, behavior selection based on rewards is closely related to the neural mechanisms of the basal ganglia.

The neuromodulator dopamine plays a central role in these processes, produced in the VTA and substantia nigra pars compacta (SNc) of the basal ganglia. Dopamine is known

to be involved in various neural functions, such as rewards, pleasure, and motor control. In particular, the dopaminergic neurons of the basal ganglia have the role of transmitting signals of reward prediction error, regulating the release of dopamine according to whether the reward prediction is realized or not (Cohen et al. 2012).

While the deep relationship between rewards and dopamine has been elucidated by many studies, there are still many questions remaining regarding the hippocampus and dopamine.

1.3 Hippocampus and Dopamine

Up until now, research has been conducted on the hippocampus and dopamine in spatial navigation. Morris and colleagues investigated the role of dopamine released in the hippocampus through pharmacological experiments. They trained rats on two tasks: one where the reward location did not change even if the environment in the open field changed, and another where the reward location changed as the environment changed. When they injected an antagonist (SCH23390) into the dorsal hippocampus of rats to prevent dopamine receptors there from taking up dopamine, it was found that the rats' behavioral response to changes in the reward location worsened. From this, it is believed that dopamine in the hippocampus plays a necessary role in behaviors adapted to environmental changes (Retailleau and Morris 2018).

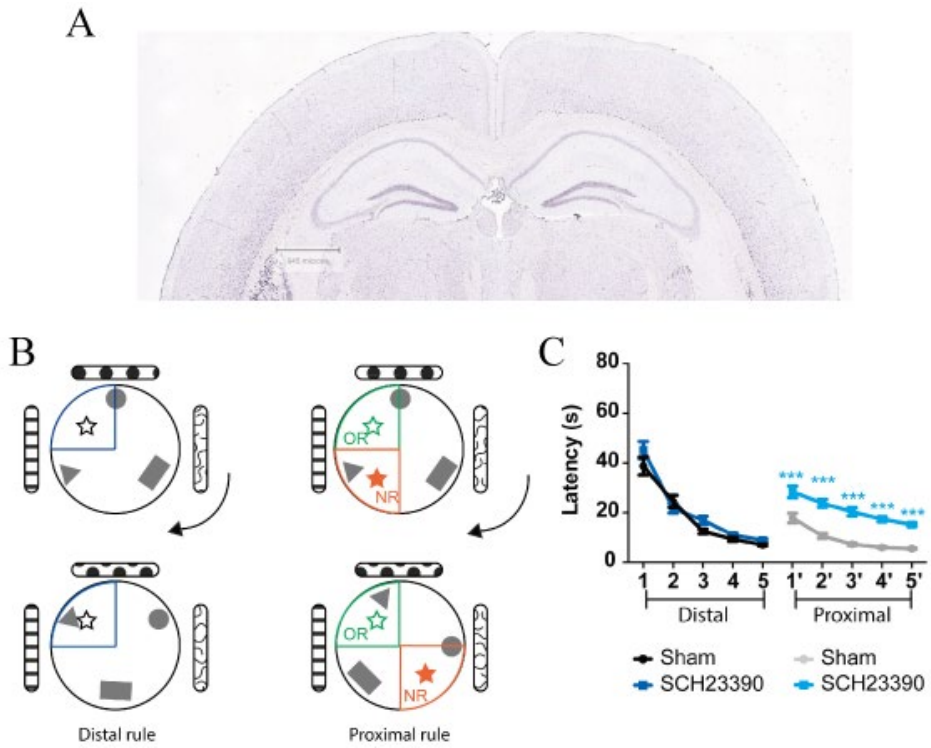

Figure 1. Inhibition of Dopamine Receptors Impedes Response to Changes in Reward Location.

(A) Expression of D1 receptor in adult mouse brain. Allen Mouse Brain Atlas, https://mouse.brain-map.org/gene/show/13267. (B) In a circular open field, three types of objects (a gray circle, triangle, and square) and a reward are placed. The reward is indicated by a star symbol. The band outside the open field represents external patterns. The open field is free to rotate, and the objects inside follow this rotation. Under the Distal rule, the open field rotates, but the reward location does not change despite changes in the positions of the internal objects. Under the Proximal rule, when the open field rotates, the reward location also rotates. Old Reward (OR) indicates the reward location during the Proximal rule, and New Reward (NR) indicates the reward location during the Proximal rule. The time it takes for a rat to reach the reward after being placed in the open field is measured, and this is done in 10 trials per day. (C) Time taken by rats to reach the reward when dopamine receptors in the dorsal hippocampus are blocked. Control group (physiological saline injected, black and gray, n=12), SCH23390 group (blue and light blue, n=13). Distal rule, day 1-5. Proximal rule, day 1'-5'. Physiological saline or SCH23390 is injected during the Proximal rule. Group comparison by Two Way Repeated Measures ANOVA followed by Sidak's test, *** $p < 0.001$.

This figure is reproduced with permission from Retailleau & Morris, 2018.

On the other hand, researchers like McNamara and Kramar have conducted a study using optogenetics to show that VTA dopamine inputs in the hippocampus are important for the stabilization of spatial memory. McNamara administered channel rhodopsin to the VTA of DAT-IRes-Cre mice and implanted optical fibers in the dorsal hippocampus to selectively excite VTA dopaminergic neurons in the hippocampus. In a hippocampus-dependent spatial learning task, while mice were exploring a maze, the dopaminergic neurons projecting from the VTA to the hippocampus were continuously excited. Although there was no significant difference compared to the condition without light stimulation during learning, when the same task was repeated one hour after learning, the mice with excited VTA dopaminergic neurons through optogenetics ran a shorter route to the reward location compared to mice without such stimulation (McNamara et al. 2014).

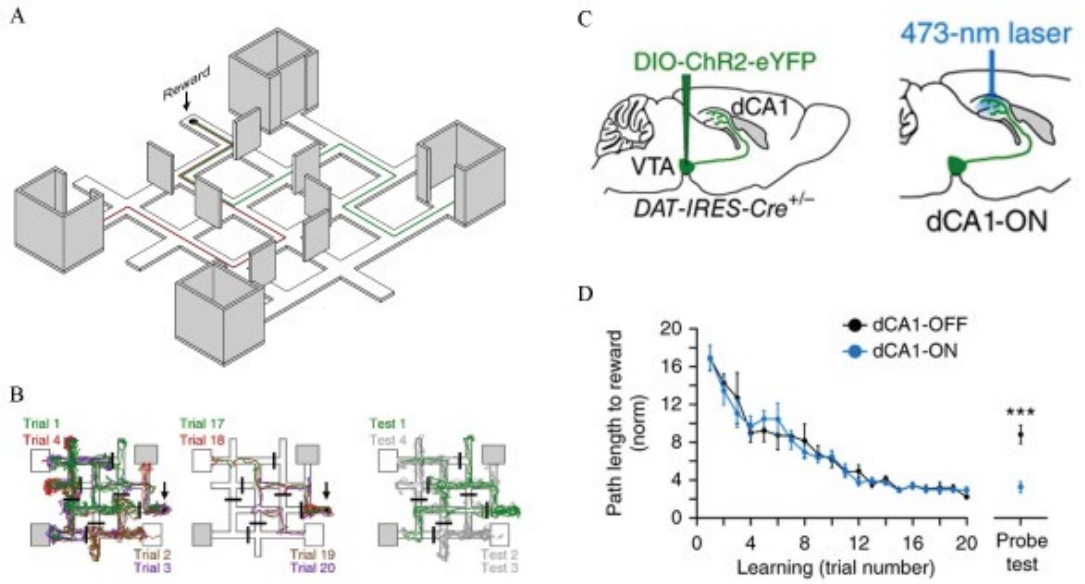

Figure 2. Fixed Reward Location Spatial Navigation Task

(A) The maze used in the experiment. There are four starting positions, but only two are chosen, with the start from either one. The two starting positions are selected to be the farthest apart. The white board is the path for the mouse, and the gray board acts as a wall, with only one path to the reward. The red and green lines in the figure show the shortest path from each starting position to the reward location. (B) This navigation task was conducted 20 times, followed by four test trials one hour later. The white box indicates the starting position, which is chosen randomly. The black solid line represents the wall, and the black arrow points to the reward location. In the test trials, no reward is given, but the goal's location is the same as the reward location during learning. The movement trajectories of the mouse in each trial are indicated in corresponding colors. (C) Injection of DIO-ChR2-eYFP into the VTA of DAT-IRES-Cre mice. This allows selective excitation of VTA dopamine inputs in the dorsal hippocampus by stimulating with blue laser light. (D) The graph shows the running distance to the reward location for the group continuously stimulated in the dorsal hippocampus (blue) and without stimulation (black) during learning of the spatial navigation task. There is no effect of light stimulation during learning, but in the Probe test conducted one hour after the end of learning, the group with light stimulation ran a shorter route to the reward location.

This figure is reproduced with permission from McNamara et al. 2014.

Additionally, Kramar and colleagues have revealed that VTA dopaminergic neurons in the dorsal hippocampus control the long-term memory of appetitive and aversive memories at the point of 12 hours post-learning (late consolidation) (Kramar et al. 2021). These studies suggest that VTA dopaminergic neurons inputting to the hippocampus play an important role in the stabilization of memory.

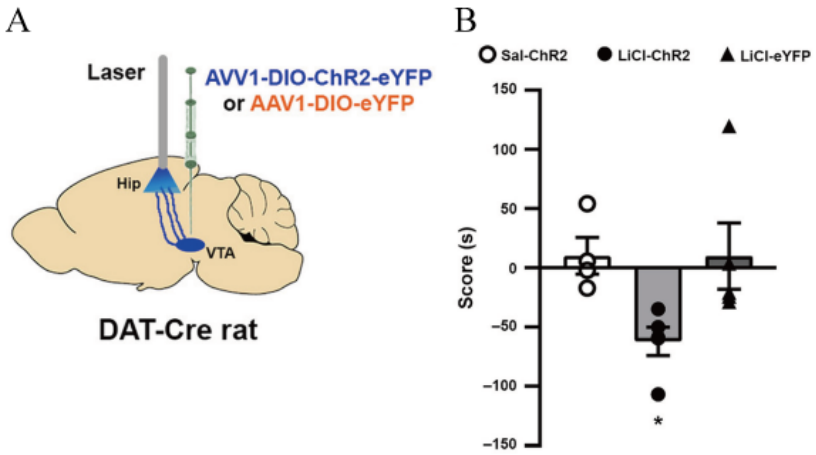

Figure 3. Dopaminergic input from the VTA to the hippocampus is important for memory stabilization.

(A) Populations of DAT-Cre rats were created, into which either ChR2 or eYFP was injected in the VTA. In an experimental setting with two types of open fields connected together, each with a different internal structure, rats were exposed to lithium chloride (LiCl) as an aversive stimulus while staying in one of the fields. This led to the rats developing an aversion to the space where LiCl was administered. After this learning process, 12 hours later, blue light stimulation was continuously applied for one hour in the home cage, with pulses of 50 Hz, 10 ms, turning on and off every 30 seconds.

(B) Seven days after the stimulation, when the rats were placed back in the same experimental environment as during learning, it was found that only the group injected with ChR2 and administered LiCl significantly avoided the space where LiCl was administered.

This figure is reproduced with permission from Kramar et al. 2021.

In summary, it is understood that dopamine within the hippocampus regulates responses to changes in goal locations during goal-directed navigation, and that excitation of VTA dopaminergic neurons is important for the stabilization of memory. However, the impact of VTA dopamine input on the hippocampus during goal adaptation in spatial navigation remains unclear.

Chapter 2. Aim of this study

To investigate the role of VTA dopamine input to the hippocampus during goal-directed navigation behavior, three types of experiments are necessary. The first is an experiment that selectively destroys dopaminergic neurons in the VTA. After training mice on a task where they receive rewards at the same location, damage to the VTA dopaminergic neurons is induced, and differences in learning and behavior before and after the damage are examined. This allows for consideration of the role played by VTA dopaminergic neurons. The second is an experiment that inhibits dopamine receptors in the hippocampus. In this experiment, an inhibitor (SCH23390) is injected into the dorsal hippocampus, and behavioral experiments are conducted. Although similar to the experiments conducted by Morris and others, this research uses a circular maze instead of an open field to exclude the possibility of mice accidentally reaching the reward location. Since it differs from previous studies, it is necessary to conduct this experiment in the context of this research. The third is an interventional experiment that excites VTA dopamine inputs within the hippocampus. McNamara and others have conducted this in tasks where the reward location is fixed, but not in cases where the reward location changes. Therefore, in this research, we will examine how behavioral performance

changes when VTA dopamine input within the hippocampus is excited in tasks where the reward location changes.

By conducting these three experiments and examining their results, we will investigate the impact of VTA dopamine input to the hippocampus during spatial navigation in the context of goal adaptation.

Chapter 3. Materials and Methods

3.1 Animals and housing conditions

Male and female DAT Cre recombinase (DAT-IRES-Cre) mice (Jackson Laboratory, stock number 006660 (Zhuang et al. 2005)) and C57BL/6J mice aged approximately 6 months at the start of the experiments were used. The mice were individually housed in separate cages, with environmental conditions maintained at a temperature range of 24–26ºC and a consistent 12-hour light/dark cycle. Experimental procedures were performed exclusively during the light phase. The body weight of each animal was adjusted to approximately 80% of their respective body weight ad libitum. While unrestricted access to water was provided, food intake was carefully controlled. Cages and housing conditions were refreshed weekly. All procedures in this study were approved by the Institutional Animal Care and Use Committee of Doshisha University.

3.2 Surgical procedures

For the lesion experiment, the mice were anesthetized using isoflurane (2%, Mylan EPD Inc., PA, USA), and a 6-hydroxydopamine (6-OHDA) solution (4 mg/ml; Sigma-Aldrich, 162957) was prepared in 0.1% L-ascorbic acid dissolved in saline (Otsuka Normal Saline, Otsuka Pharmaceutical Factory, Japan). The 6-OHDA solution was bilaterally injected at

a volume of 0.5 μl into the VTA through the pre-implanted cannula at stereotaxic coordinates: AP: -3.1 mm, ML: ±0.4 mm, and DV: -4.2 mm (Figure 4). Following injection, the animals were allowed a recovery period of at least 1 week before conducting the post-lesion behavioral tests. In the control group, saline was bilaterally injected into the VTA using the same procedure as that used for the 6-OHDA injection.

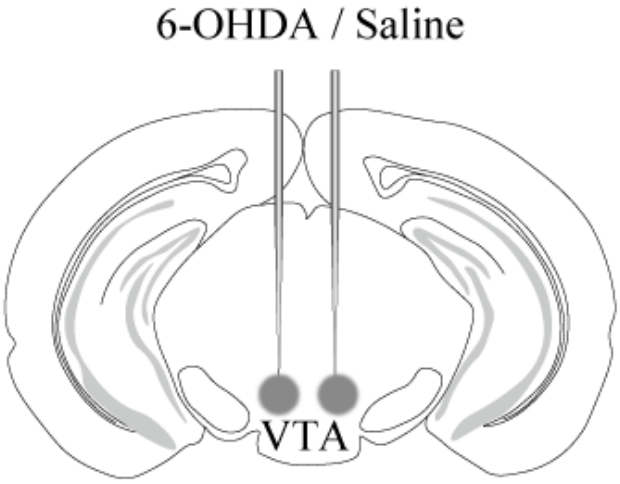

Figure 4. Schematic representation of the selective lesion method for VTA dopamine neurons.

Schematic representation of a coronal section of the mouse brain. The gray circles indicate the location of the VTA. Cannula tips were implanted to target both sides of the VTA. After injecting 6-OHDA or saline, the cannula was removed, and the mouse's scalp was sutured.

This figure is adapted from Tamatsu et al. 2023.

For the micro-infusion experiment, mice were anesthetized with isoflurane to selectively block the dopamine D1 receptor in the dorsal hippocampus. To implant a cannula in both hemispheres of the dorsal hippocampus, two cannulas (diameter 22G, 5.0 mm long, PlasticsOne, TX, USA) were bilaterally placed at coordinates AP: -2.4 mm, ML: ±2.5 mm, and DV: -1.4 mm using a bilateral internal cannula (C232G, PlasticsOne, TX, USA) (Figure 5).

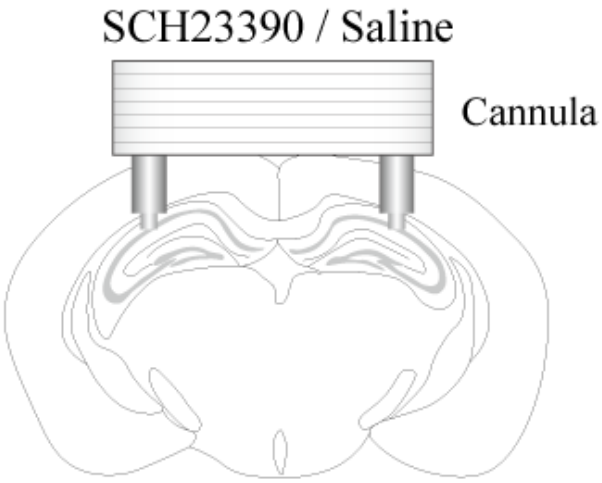

Figure 5. Schematic diagram of cannula placement for the micro-infusion experiment.

This schematic represents the implantation of a cannula into the dorsal hippocampus for the injection of SCH23390 or saline. Coordinating with the lesion experiment's location, holes were drilled, and the cannula was placed. Subsequently, the cannula and skull were secured using dental cement to ensure the cannula remained in place.

This figure is adapted from Tamatsu et al. 2023.

For the optogenetics experiment, to selectively activate the axons of the VTA dopaminergic neurons projecting to the dorsal hippocampus, mice were anesthetized with isoflurane, and six holes were drilled into their skulls for anchor-screw placement. The anchor screws were then installed. Additionally, two holes were made in the VTA for AAV administration, followed by bilateral injection of 0.8 μl AAV (pAAV-Syn-FLEX-rc [ChrimsonR-tdTomato], titer 8.5×10^{12} genome copies/mL, Addgene, MA, USA) at each site. To implant an optical fiber in both hemispheres of the dorsal hippocampus, two optical fibers (FT200EMT, diameter 200 μm, pure silica material, THORLABS, NJ, USA) were bilaterally placed at coordinates AP: -2.0 mm, ML: ±1.9 mm, and DV: -0.8 mm using a custom adapter designed in-house using Onshape (Parametric Technology Corporation, MA, USA) and printed with a 3D printer (Form 2/3, Formlabs Inc., MA, USA) (Figure 6).

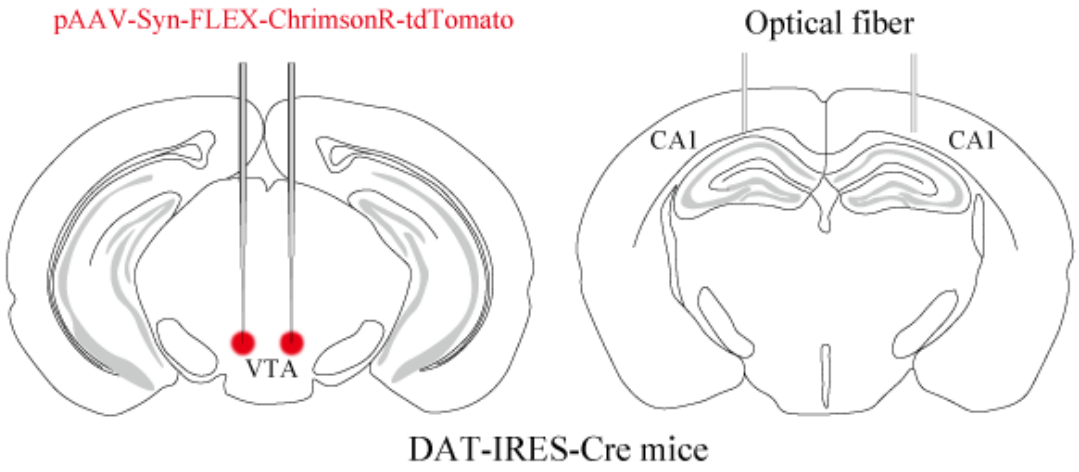

Figure 6. Schematic representation of optical fiber implantation surgery.

Initially, AAV was administered to the VTA using a method similar to that of the lesion experiments (left). Subsequently, optical fibers were implanted bilaterally in the dorsal hippocampus, and the skull, anchor screws, and adapter were securely bonded and fixed in place using dental cement(right).

This figure is adapted from Tamatsu et al. 2023.

For concurrent optogenetic and fiber photometry experiments, 0.8 μl AAV (pAAV-Syn-FLEX-rc [ChrimsonR-tdTomato], titer 8.5 × 10^{12} genome copies/mL, Addgene) was bilaterally injected into both hemispheres of the VTA. In addition, 0.8 μl AAV (AAV.CamKII.GCaMP6f.WPRE.SV40, titer 8.5 × 10^{12} genome copies/mL, or pAAV-hsyn-$GRAB_{DA2h}$, titer 8.5 × 10^{12} genome copies/mL, Addgene) was injected into the unilateral (GCaMP6f or $GRAB_{DA2h}$) or bilateral (GCaMP6f on one side and $GRAB_{DA2h}$ on the other) hippocampal CA1 (AP: -2.0 mm, ML: ±2.0 mm, and DV: -1.1 mm) for fiber photometry. This was followed by implantation of a TeleFiOpto cannula (diameter 400 μm, Bio Research Center, Co., Ltd.) and fixation with dental glue (RelyX Unicem 2, 3M, MN, USA). The surface of the glue was black-coated with dental cement kneaded with carbon powder (Sigma-Aldrich, 484164) to prevent the optogenetically stimulated light and fiber photometry excitation light from leaking through the translucent glue (Figure 7).

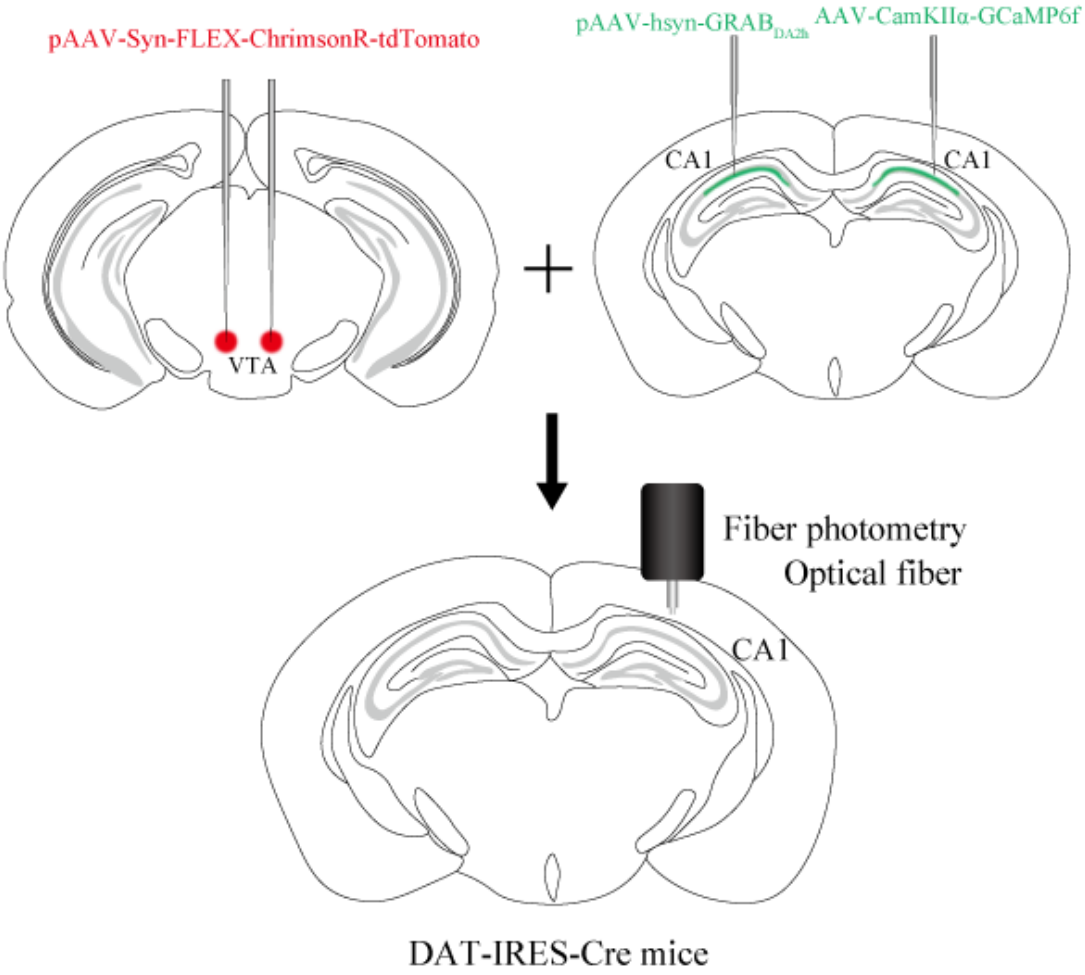

Figure 7. Schematic representation of the experimental setup for concurrent optogenetic and fiber photometry investigation.

Bilateral injection of pAAV-Syn-FLEX-ChrimsonR-tdTomato into the VTA of DAT-IRES-Cre mice was performed to generate DATVTA mice (top left). AAV-CamKIIα-GCaMP6f and/or pAAV-hsyn-GRAB$_{DA2h}$ were unilaterally injected into the dorsal hippocampus of DATVTA mice (top right). A fiber-optic was unilaterally inserted into the dorsal hippocampal CA1 of DATVTA mice, and simultaneous stimulation of VTA dopaminergic axons was performed to record calcium or dopamine signals (bottom).

This figure is adapted from Tamatsu et al. 2023.

3.3 Apparatus

A reconfigurable maze was used for behavioral testing, as described in a previous study(Hoshino et al. 2020; Sawatani et al. 2022). The maze contained various objects such as mushroom-shaped, cylindrical, and triangular prisms. A sensor system was integrated to record the passage and poking timing of the mice, which were then sent to a computer via serial communication.

3.4 Behavioral testing environment

A total of 54 mice were assigned to groups: control, dopamine-deficient, pharmacological intervention, optogenetic stimulation, and concurrent optogenetics and fiber photometry. The control group consisted of 4 C57BL/6J mice and 3 DAT-IRES-Cre mice; the dopamine-deficient group, 12 C57BL/6J mice; the pharmacological intervention group, 10 C57BL/6J mice; the optogenetic stimulation group, 8 DAT-IRES-Cre mice (2 and 3 mice used for short and long stimulation, respectively, and 3 mice used for both short and long stimulations); and the concurrent optogenetic and fiber photometry group, 17 DAT-IRES-Cre mice (6 mice expressing GCaMP6f unilaterally, 3 mice expressing $GRAB_{DA2h}$ unilaterally, and 8 mice with GCaMP6f expressed on one side and $GRAB_{DA2h}$ on the other). For the optogenetic stimulation group, unfortunately,

due to an incident where mice fell from the elevated maze, the optical fiber adapter sustained damage, rendering the continuation of the experiment impossible.

All behavioral experiments were conducted in a soundproof room with minimal human involvement during the experiments. A 10 mg AIN-76A Rodent Tablet (Test Diet, O'HARA & CO., LTD., Japan) was used as a food reward. Feces and urine were removed between sessions, and maze pathways were lightly cleaned with 70% ethanol. A camera was installed above the maze to record the behavior of the mice during the task.

3.5 Behavioral paradigms

Behavioral experiments were performed using a reconfigurable maze platform. The maze comprised 8 paths, 4 linear and 4 curved, each measuring 4 cm in width and 40 cm in length, forming a circular maze with a total length of 320 cm. The feeding stations were positioned in the north, south, east, and west. Infrared-blocking sensors were installed 15 cm from each feeding station. The passage through which the mouse traveled was identified based on the sensor data. Transparent acrylic gates were installed between the passages near the feeding stations to prevent the mice from retracing their steps after obtaining food. Three distinct landmark objects were placed within the circular maze: a mushroom-shaped object (an upper hemisphere with a diameter of 18 cm and a lower

cylinder with a diameter of 8 cm and a height of 13 cm), a rectangular prism (11 cm × 11 cm × 28 cm), and a triangular prism (an equilateral triangle with 18 cm sides and a height of 24 cm).

The opening and closing of the gates and food administration were controlled using a microcontroller (Arduino MEGA 2560). The Arduino temporarily stored the timings of sensor blockage and nose poking at the feeding stations, simultaneously transferring the data to a host computer via serial communication. The mice were trained in two types of behavioral tasks, namely, a fixed-reward location task and a changing-reward location task, which involved altering the placement of rewards or landmark objects. In both tasks, the start position remained consistent throughout the experiment, and the mice were trained to run in a clockwise direction. Before undertaking the fixed or changing reward location tasks, the mice were first habituated to the maze for 1 week, followed by 5 days of training for the fixed reward location task. One session was defined as either 10 laps of the circular maze or 15 minutes from the start, whichever came first. The session was terminated when the mouse escaped the maze. In the optogenetic experiments, one session was defined as the completion of 10 laps of the circular maze by the mouse.

3.6 Behavior task

In this study, we investigated the behavioral responses of mice in a circular maze, particularly their ability to adapt to fixed and changing reward locations. The experiments were conducted in a soundproof room, and the reward locations in the maze were set at four points: east, west, south, and north. The reward was pellet food from a single dispenser. To evaluate the mice's adaptation to changing reward locations, we designed two tasks: a fixed reward location task and a changing reward location task. In both tasks, the mice were trained to find the reward relying only on distant objects inside the soundproof room. The researchers disrupted cues from proximal landmarks by randomly rearranging three conspicuous objects in the maze with each session (Figure 8).

3.6.1. Fixed reward location task

Throughout the experiment, the reward location remained constant across sessions, whereas the arrangement of landmark objects placed within the maze was randomly altered.

3.6.2. Changing reward location task

In each session, the reward location shifted with changes in the arrangement of landmark objects. Adjustments were made to ensure no associations existed to avoid any preserved

relative relationship between landmark objects and reward locations when randomly changing positions.

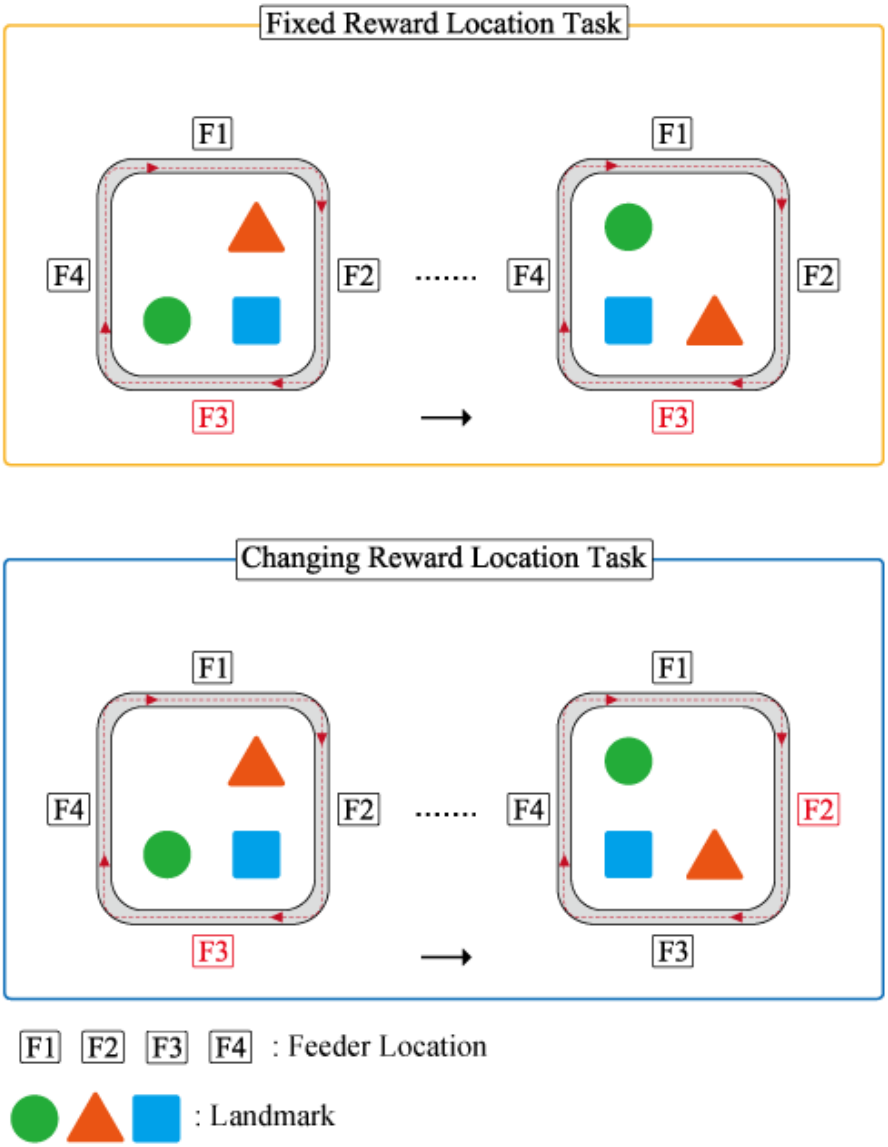

Figure 8. Maze configuration for spatial learning tasks in mice.

(A) Maze schematics. Top: Example configuration for the fixed reward location task, with the rewarded feeder (F3) remaining in a fixed location after each randomized rotation of the landmark objects. Bottom: Example configuration for the changing reward location task, in which the rewarded feeder (F3) is relocated after each randomized rotation of the landmark objects.

This figure is adapted from Tamatsu et al. 2023.

3.7 Infusion protocol

SCH23390 (D054, Sigma-Aldrich, 5mg/ml concentration diluted in saline) or saline was infused using a Hamilton syringe (88411, Hamilton, CA, USA) coupled with a motorized stereotaxic microinjector (IMS-20, Narishige, Japan). The infusion was administered bilaterally at a rate of 0.05 µl/min, with a total volume of 0.6 µl per hemisphere (1.2 µl bilaterally) according to previous studies (O'Carroll et al. 2006; Retailleau and Morris 2018). The cannula was removed 1min post-infusion, and the task was initiated 20 min after the cessation of anesthesia.

3.8 Optogenetic stimulation protocol

For optogenetic stimulation during a task involving dynamic reward locations, light with a wavelength of 595 nm was emitted at a frequency of 20 Hz at ~2.5 mW/mm^2 at the fiber implant tip, employing a duty cycle of 4/5 for 1s from the tip of the optical fiber situated directly above the CA1 cell layer within the dorsal hippocampus (light source: Fiber-Coupled LED 595 nm [M595F2]; THORLABS). The experiments were conducted using no light (no-stim) and three distinct light exposure timings (pre-stim, post-stim, and opposite-stim).

Pre-stim: Illumination commenced immediately after the mouse traversed the infrared-blocking sensor positioned 15 cm in front of the reward location.

Post-stim: Illumination ensued directly after the mouse performed a nose poke to obtain the reward.

Opposite-stim: Illumination was initiated immediately after the mouse traversed the infrared-blocking sensor positioned 15 cm before the feeder opposite to the reward location (e.g., the south feeder when the north feeder served as the reward location).

3.9 Concurrent optogenetics and fiber photometry protocol

Fiber photometry was performed using a wireless fiber photometry and optogenetics system (*TeleFiOpto*; Bio Research Center Co., Ltd., Japan). For optogenetic stimulation, light with a wavelength of ~620 nm was delivered at a frequency of 20 Hz with 10 ms or 40 ms pulses at ~1 mW/mm^2 at the fiber implant tip in 10s sessions consisting of 1s of stimulation followed by 9s of no stimulation. Simultaneously, the mice freely roamed in an open field (diameter: 31 cm, height: 17 cm). This protocol was repeated for 30min, comprising 180 sessions. Fiber photometry recordings were used to acquire fluorescence signals at an excitation wavelength of approximately 470 nm during optogenetic stimulation.

3.10 Analysis

Timestamps about the passage of infrared-blocking sensors and nose poke timings measured during the behavioral tasks were temporarily stored on an Arduino microcontroller. After completing all tasks, the data were transferred to a computer via serial communication. Communication between the Arduino microcontroller and the PC was facilitated using MATLAB (Mathworks, MA, USA). For the lesion experiments, the correct response rate, rule learning rate, and number of laps were calculated for each session. The correct response rate was defined as the number of laps in which the animal only chose a reward-providing feeder divided by the total number of laps. The rule learning rate was defined as the number of laps in which the animal chose only one of the four available feeders in each lap, regardless of whether it was a reward-providing feeder, divided by the total number of laps. Four sessions were conducted daily, and the average values were calculated for each subject. In the optogenetic experiments, the correct response and rule learning rates were calculated in the same manner as that in the lesion experiments. In the post-stim trials, the correct response and rule learning rates were calculated starting from the lap following reward acquisition.

The running speed was determined by dividing the fixed distance (15 cm) by the time elapsed for each mouse to cross the sensor and poke its nose at the reward location. Fiber photometry data were recorded using *TeleFipho* software (BioResearch Center, Co., Ltd., Japan) at a sampling rate of 100 Hz to capture both raw photometry data and event data for optogenetic stimuli. These data were analyzed using *pMAT* (Bruno et al. 2020) to obtain the % $\Delta R / R_0$ and Z-scores of the peri-event time histograms across the 180 experimental sessions. The time window for this analysis was 1s before and 8s after the start of the stimulation, with a baseline sampling window of 1s immediately before the start of the stimulation and a bin constant of 0.1s. The average % $\Delta R / R_0$ of GCaMP6f and $GRAB_{DA2h}$ responses by stimulus duration was calculated during stimulation (1s from the onset of the stimulation) and early (2–5s after the onset of the stimulation) and late (5–8s after the onset of the stimulation) phases of post-stimulation, respectively. We also counted the number of experimental sessions where the Z-score exceeded 1.96 during the 1.5s epoch commencing 0.05s after the start of the stimulation.

Behavioral event classification was performed using concurrent optogenetic and fiber photometry experiments. Using *DeepLabCut*^{TM} (Mathis et al. 2018), we precisely tracked six joint locations in mice, notably in the neck. Our study primarily utilized neck-point data to distinguish between behavioral events. We defined ambulation events as those

when the neck point-derived speed exceeded an average of 2 cm/s for a sustained half-second(Kravitz et al. 2010). Conversely, immobility events emerged during continuous periods with speeds below 2 cm/s lasting for at least 1s. The remaining movements that did not fulfill the ambulation or immobility criteria were classified as “fine movement events,” reflecting their nuanced nature.

3.11 Histological assessment

After mice were euthanized through a pentobarbital sodium overdose and subsequently perfused with formalin, their brains were frozen and sectioned coronally at 40-μm thickness using a sliding microtome. The sections were divided into six interleaved sets for immunostaining or Nissl staining with cresyl violet (Sigma-Aldrich, St. Louis, MO, USA; C5042-10G). Free-floating sections were pretreated with 3% hydrogen peroxide and incubated overnight with a primary mouse anti-tyrosine hydroxylase antibody (1:1000; Merck Millipore, MAB318) to assess the dopaminergic neuronal loss. The sections were incubated with the secondary antibody biotinylated donkey anti-mouse IgG (1:100; Jackson ImmunoResearch Inc., 715-065-151), followed by incubation with an avidin-biotin-peroxidase complex solution (1:100; Vector Laboratories, PK6100). Immunoreactivity was visualized using 3-3′ diaminobenzidine tetrahydrochloride

(Dojindo Laboratories, 349-00903). The degree of dopaminergic cell loss was estimated by comparing cell counts across representative sections of the VTA and SNc – the most rostral, caudal, and intermediate sections – between lesioned and non-lesioned control mice. The cells were manually counted using a microscope, and images were acquired for further analysis (Table 1). The acquired images were processed and analyzed using ImageJ or Adobe Photoshop software for cell identification and quantification. Free-floating sections were incubated overnight with a primary rabbit anti-tyrosine hydroxylase antibody (1:200; Merck Millipore, AB152) to evaluate the viral expression cells. Subsequently, the samples were incubated with the secondary antibody, Alexa Fluor 488-conjugated cross-adsorbed goat anti-rabbit IgG (H+L) (1:100; Invitrogen, A11008). Fluorescent images of TH and ChrimsonR-fused tdTomato were acquired using a fluorescence microscope (BZ-X800L/BZ-X810, BZ-H4XD multistack module and BZ-H4XF sectioning module [Keyence Co., Osaka, Japan]). The acquired images were processed and analyzed using ImageJ or Adobe Photoshop software.

Table 1 VTA and SNc cell counts.

Dopaminergic neuron deficient mice		
mice	VTA	SNc
#1	151	1852
#2	204	2174
#3	230	1907
#4	72	1818
#5	175	1793
#6	74	1801
#7	200	2124
#8	253	2083

Non-deficient control mice		
mice	VTA	SNc
#1	883	4313
#2	573	3696
#3	661	4288
#4	541	4268
#5	779	3561
#6	899	3700
#7	981	4067

3.12 Statistics

In the lesion experiments, differences in the correct response and rule learning rates between the saline-infused and 6-OHDA-infused VTA groups were assessed using a two-way mixed ANOVA. In the pharmacological experiments, differences in the number of laps between the saline-infused and SCH23390-infused groups were assessed using a two-way repeated measures ANOVA and differences in the correct response and rule learning rates between the wild-type and saline-infused groups were assessed using Wilcoxon rank-sum test. In the optogenetic experiments, the control group without light stimulation (control-stim) was compared with the groups with pre-stimulation, post-stimulation, and opposite-stimulation using a two-way repeated-measures ANOVA. Both two-way mixed ANOVA and two-way repeated-measures ANOVA were performed using the ranova function in MATLAB. In the concurrent optogenetic and fiber photometry experiments, single or multiple Wilcoxon signed-rank tests with Bonferroni corrections were performed using the sign-rank function in MATLAB.

The shuffling distribution of the correct and rule learning rates was calculated by randomly shuffling the trial number 1000 times. We confirmed that the mice learned each task if the correct rate or rule learning rate exceeded the entire distribution ($P < 0.001$).

Chapter 4. Results

4.1 Learning of fixed and changing reward location tasks

In the fixed reward location task, the mice were trained to locate the reward at a fixed location. We calculated the correct response rate, defined as the number of laps in which the animal only chose a reward-providing feeder divided by the total number of laps. The mice achieved an average correct response rate of 80% on the second day of training, with all mice exceeding chance levels defined by the shuffled distribution, confirming their ability to learn the reward location in this task (Figure 9A). A previous study performed by blocking dopamine receptors in the hippocampus showed that dopamine was involved in changing reward location information (Retailleau and Morris 2018). Building on this finding, we trained mice to perform a changing reward location task in which only the modification from the fixed reward location task involved randomly changing the position of the reward. Mice maintained an average of 50% correct response rate after 4 days of training, with all wild-type mice exceeding chance levels defined by the shuffled distribution. This indicated that mice could also learn the changing reward location task (Figure 9B). On day 1, the mice could not update the reward location information. However, from day 2 onward, they engaged in exploratory behaviors, nose-poking multiple dispensers to identify the reward location, and gradually selected only

one specific reward location. Mice adaptation to reward location rules did not necessarily correlate with the correct response rate. In addition to the correctness, we also calculated the rule-learning rate (i.e., the number of laps in which the animal chose only one of the four available feeders in each lap, regardless of whether it was a reward-providing feeder, divided by the total number of laps) to assess rule-learning abilities. In wild-type mice, the rule learning rate progressively increased over 4 days, ultimately reaching an average of 50%. All mice exceeded chance levels defined by the shuffled distribution, showing that they could learn the rule of changing the reward location task (Figure 9).

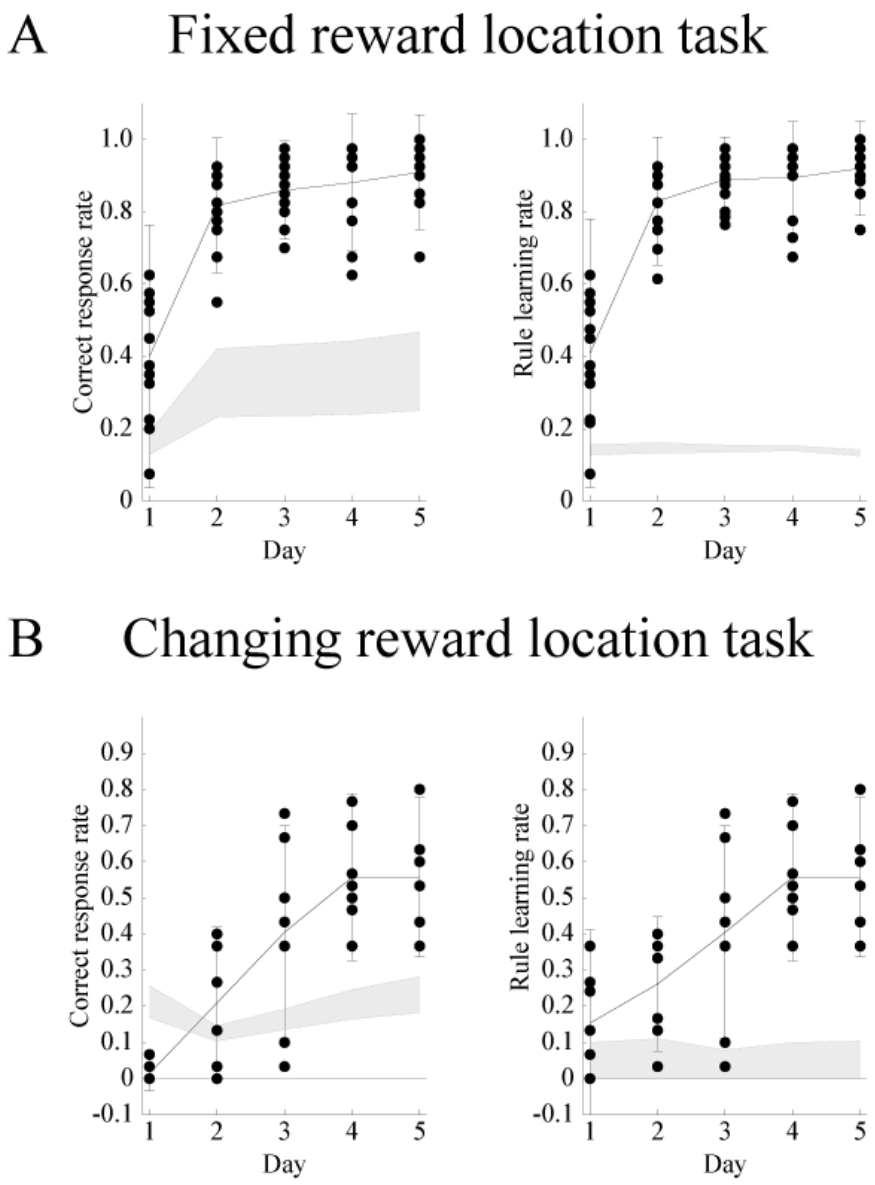

Figure 9. Behavioral paradigm for spatial learning tasks in mice.

(A) Correct response rate (left) and rule learning rate (right) during the fixed reward location task performance. The gray shaded area represents the shuffled distribution of both rates, which exceed the chance level from day 2 onward. (B) Correct response rate (left) and rule learning rate (right) during the changing reward location task performance. The gray shaded area represents the shuffled distribution of both rates, which exceed the chance level from day 4 onward. The dots represent raw data points for individual mice, while the graph indicates mean ± standard deviation (SD).

This figure is adapted from Tamatsu et al. 2023.

4.2 Effect of loss of dopaminergic neurons on reward location persistence and updating

We selectively lesioned the dopaminergic neurons of mice using the neurotoxin 6-OHDA (Figure 10A) and subjected them to fixed and changing reward location tasks (Figure 10B). Mice administered with saline instead of 6-OHDA were used as controls. Dopaminergic neuron loss in the VTA significantly exceeded that in the SNc ($P < 0.001$, Wilcoxon signed-rank test, n = 12 mice; Figure 10C), corroborating the anticipated preponderance of deficiencies in the VTA. However, the non-trivial extent of dopaminergic loss in the SNc warrants consideration in subsequent analyses.

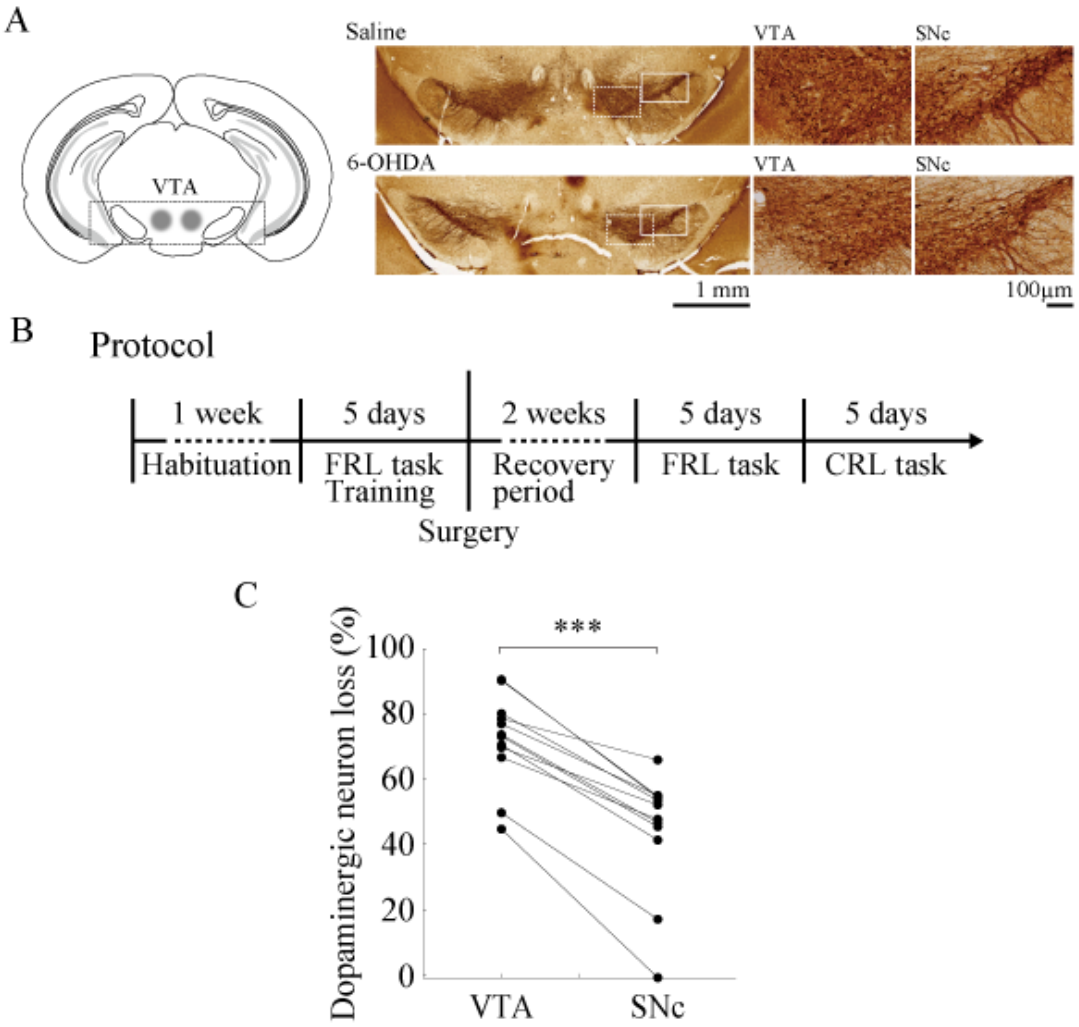

Figure 10. Dopamine deficiency alters task performance and learning in mice.

(A) Post-hoc verification of bilateral injection of 6-hydroxydopamine (6-OHDA) or saline into the VTA with cannula tips for drug injection (left). Representative tyrosine hydroxylase (TH)-stained coronal sections of saline (top)- or 6-OHDA (bottom)-injected mice are displayed on the right side. The areas within the white solid (SNc) or dotted (VTA) rectangles are presented in magnified views (right). (B) The percentage of dopaminergic neuron loss in the VTA and SNc. ***: $P < 0.001$, Wilcoxon signed-rank test, n = 12 mice. (C) Experimental timeline. Mice are habituated to the maze for 1 week, followed by 5 days of training in the fixed reward location (FRL) task. After a 2-week recovery period post-injection surgery, mice perform the FRL task for 5 days; then the changing reward location (CRL) task for 5 days.

This figure is adapted from Tamatsu et al. 2023.

We compared the total number of laps run and running speed to reach the reward location within a session between VTA/SNc dopaminergic neuron-deficient and control mice. Our data highlighted the significant influence of dopaminergic deficiency on these measures in both tasks. In the fixed-reward location task, there were significant variations in both the number of laps ($F_{1,17} = 12.8$, $P < 0.01$, Greenhouse–Geisser-corrected) and running speed ($F_{1,14} = 26.7$, $P < 0.01$) (Figure 11A). Similarly, in the changing reward location task, marked differences were noted in the number of laps ($F_{1,17} = 13.4$, $P < 0.01$, Greenhouse–Geisser-corrected) and running speed ($F_{1,10} = 39.4$, $P < 0.01$) (Figure 11B). These results were obtained from a two-way mixed analysis of variance (ANOVA) involving 7 control mice and 12 dopaminergic-deficient mice. The analysis indicated that a deficiency in VTA/SNc dopaminergic neurons significantly altered the number of laps completed and the speed at which the rewards were reached. This finding highlights the importance of dopamine levels from VTA/SNc in maintaining motivation and motor skills necessary for task execution. The fixed reward location task demonstrated significant influences of the experimental day and the interaction between dopamine deficiency and the experimental day on the outcomes of total lap run and running speed ($P < 0.05$, interaction, Greenhouse–Geisser-corrected). Conversely, the changing reward location

task showed no significant interaction effect ($P > 0.05$, interaction, Greenhouse–Geisser-corrected).

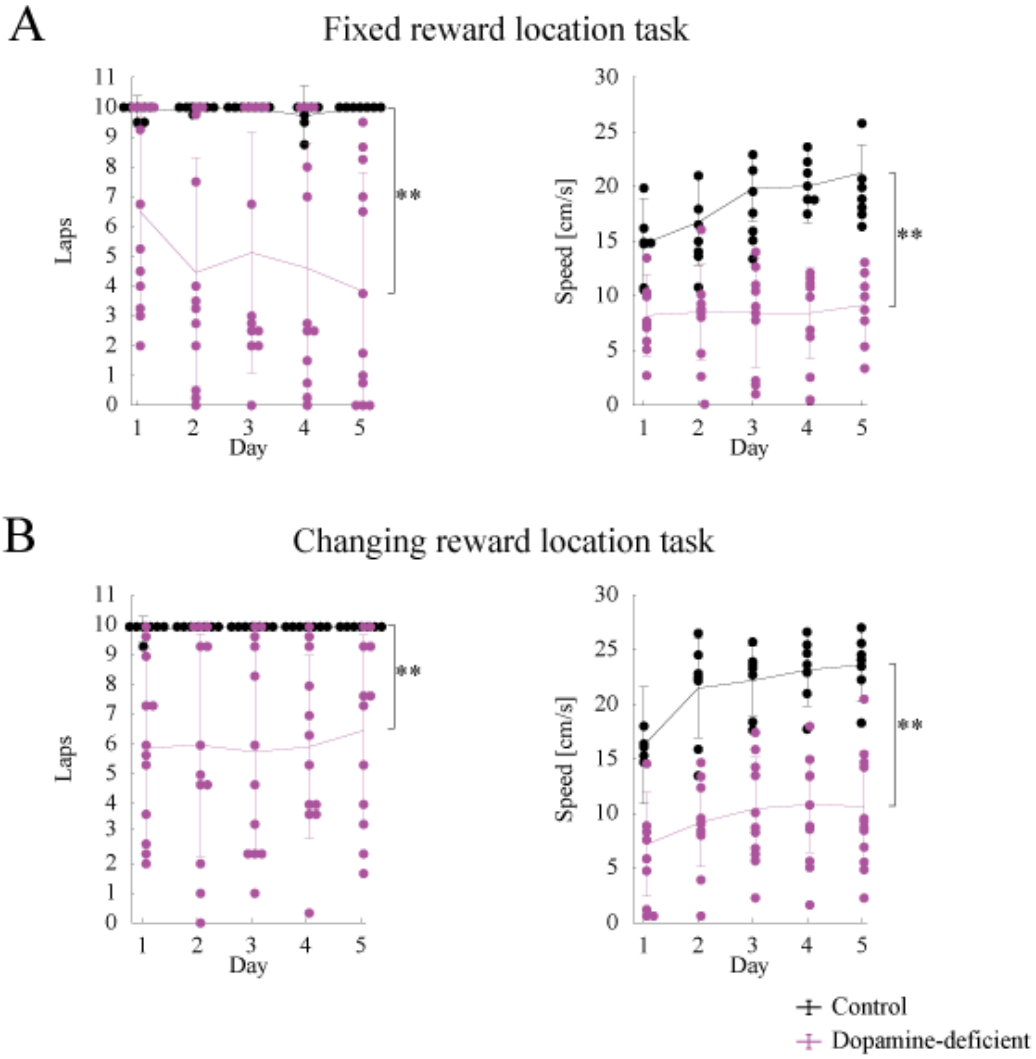

Figure 11. Dopamine deficiency decreases task performance in mice.

(A-B) The number of laps (left) and running speed to reach the reward location (right) during the fixed reward location task (A) or changing reward location task (B) performance for dopamine-deficient (purple) and non-deficient (black) mice. Dots represent individual data points for each mouse, while the graph indicates mean ± standard deviation (SD). *: $P < 0.05$, **: $P < 0.01$, two-way mixed ANOVA. n = 7 mice (control), 12 mice (dopamine deficient).

This figure is adapted from Tamatsu et al. 2023.

In the fixed reward location task, we found significant discrepancies in both the rates of correct response and rule learning (correct response: $F_{1,14} = 9.83$, $P < 0.01$; rule learning: $F_{1,14} = 7.57$, $P < 0.05$, Greenhouse–Geisser-corrected; Figure 12A). Moreover, these discrepancies were also evident in the changing-reward location task (correct rate: $F_{1,16} = 9.74$, $P < 0.01$; rule learning: $F_{1,16} = 7.51$, $P < 0.05$; Figure 12B). These findings, analyzed using a two-way mixed ANOVA, are consistent with the results of previous studies(Kramar et al. 2021; McNamara et al. 2014; Takeuchi et al. 2016) that showed that a deficiency in VTA/SNc dopaminergic neurons could contribute to the maintenance of spatial memory during the performance of tasks with a fixed reward location. Furthermore, these findings are also consistent with evidence from a previous study, which involves the blockade of hippocampal dopaminergic receptors, that shows that the release of local dopamine in the hippocampus plays a role in updating spatial goals (Retailleau and Morris 2018).

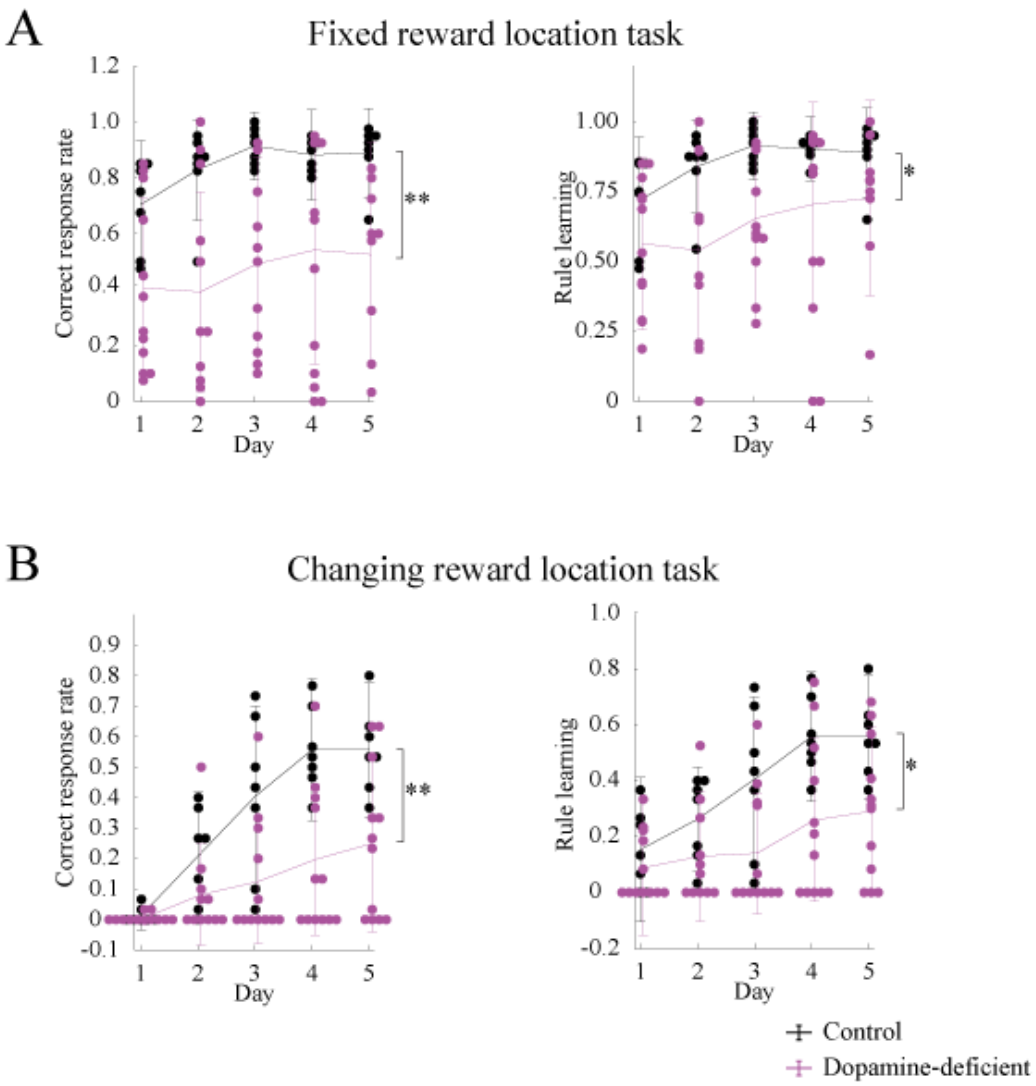

Figure 12. Dopamine deficiency decreases the ability of mice to learn tasks.

(A-B) Correct response rate (left) and rule learning rate (right) for the fixed reward location task (A) and changing reward location task (B) performance of dopamine-deficient (purple) and non-deficient (black) mice. Dots represent individual data points for each mouse, while the graph indicates mean ± standard deviation (SD). *: $P < 0.05$, **: $P < 0.01$, two-way mixed ANOVA. n = 7 mice (control), 12 mice (dopamine deficient).

This figure is adapted from Tamatsu et al. 2023.

4.3 Effect of blockade of hippocampal dopamine receptors

The association between VTA-derived dopamine and the hippocampal response in the context of reward location alterations is challenging to discern because of the significant influences on motivation, motor impairment, or both and the broad projections of VTA/SNc dopaminergic neurons (Ioanas, Saab, and Rudin 2022). This complexity underscores the challenge of making definitive interpretations. To isolate hippocampal-dependent effects from the broader projections of VTA/SNc dopaminergic neurons, we administered SCH23390, a selective dopamine D1 receptor antagonist, to the dorsal hippocampus of mice subjected to a fixed reward location task (Figure 13).

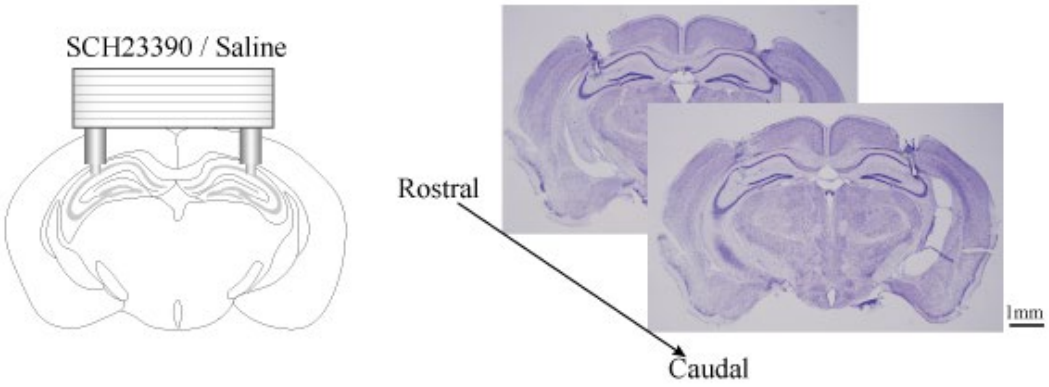

Figure 13. Representative example of Nissl-stained coronal sections of mice in pharmacological experiments.

Schematic representation of the experimental setup for pharmacological experiment. Representative Nissl-stained coronal sections of mice treated with SCH23390 were displayed on the right side.

This figure is adapted from Tamatsu et al. 2023.

Saline-administered mice served as vehicle controls. Interestingly, mice with D1 receptor blockade remained largely stationary near the feeder. There were significant differences in the total number of laps run within a session between the D1 receptor-blocked mice and the vehicle control mice ($F_{1,9} = 89.7$, $P < 0.01$, Greenhouse–Geisser-corrected) (Figure 14).

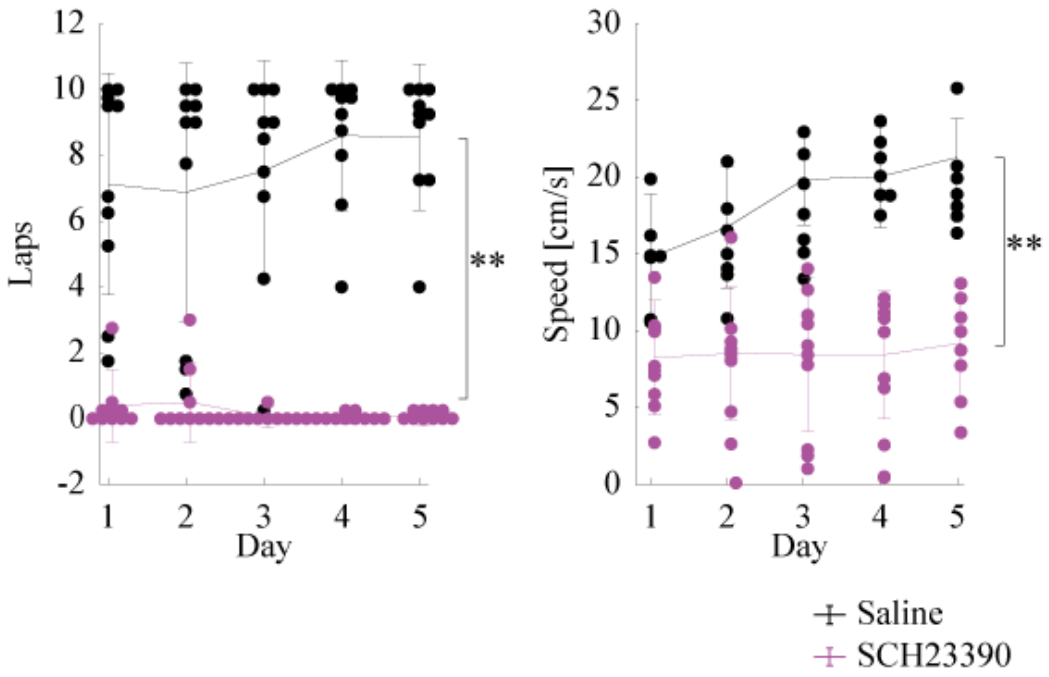

Figure 14. Blocking dopamine receptors drastically reduces task performance in mice.

The number of laps during the fixed reward location task performance for dopamine receptor-blockade (purple, SCH23390) and vehicle control (black, saline) mice. Statistical significance is determined using two-way repeated-measures ANOVA. **: $P < 0.01$, n = 10 mice.

This figure is adapted from Tamatsu et al. 2023.

These findings were derived from a two-way repeated-measures ANOVA involving 10 control and 10 dopamine receptor-blocked mice. Importantly, saline infusion did not impair task performance, as supported by comparable correct response rates and rule-learning metrics between vehicle controls and pre-operated wild-type mice (correct response: $P > 0.05$; rule learning: $P > 0.05$, Wilcoxon rank sum test; Figure 15).

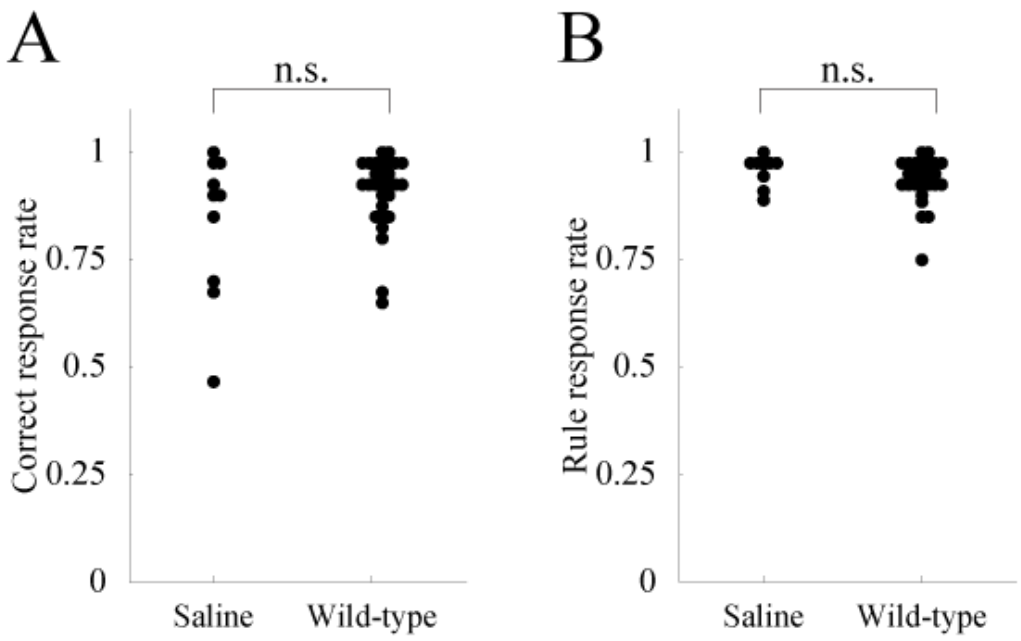

Figure 15. Saline infusion does not impair task performance.

Correct response rate (A) and rule learning rate (B) for the fixed reward location task performance of vehicle control (saline) and non-operated wild-type mice. Wilcoxon rank sum test, n.s.: $P > 0.05$, vehicle control: n = 10 mice, wild-type: n = 29 mice.

This figure is adapted from Tamatsu et al. 2023.

This unexpected result underscores the intrinsic role of dopamine in the dorsal hippocampus for sustaining the motivation and/or motor skills essential for task performance, independent of the broader VTA/SNc dopaminergic projections. Owing to the near-immobility of the dopamine receptor-blocked mice in the maze, we were unable to assess their performance in tasks involving both fixed and changing reward locations.

4.4 Optogenetic activation of the VTA-hippocampal pathway enhances reward location adaptation.

Dopamine inputs to the hippocampus originate from both the VTA and LC (Takeuchi et al. 2016; Tsetsenis et al. 2021). Thus, considering our findings, focusing on the specific activation, rather than inhibition, of the input from VTA dopaminergic neurons to the hippocampus is crucial(McNamara et al. 2014). We examined the causal relationship between VTA dopaminergic neurons expressing the dopamine transporter (DAT) and the dorsal hippocampus. A Cre-inducible viral construct encoding ChrimsonR fused to an enhanced red fluorescent protein (ChrimsonR-tdTomato) was injected into the VTA of DAT-IRES-Cre mice (Figure 16A-B). A fiber-optic tip was positioned directly above the pyramidal cell layer of the dorsal hippocampal CA1 of DAT^{VTA} mice, and orange light

was applied as an intervention. The data without light exposure were used as controls for the same group of mice.

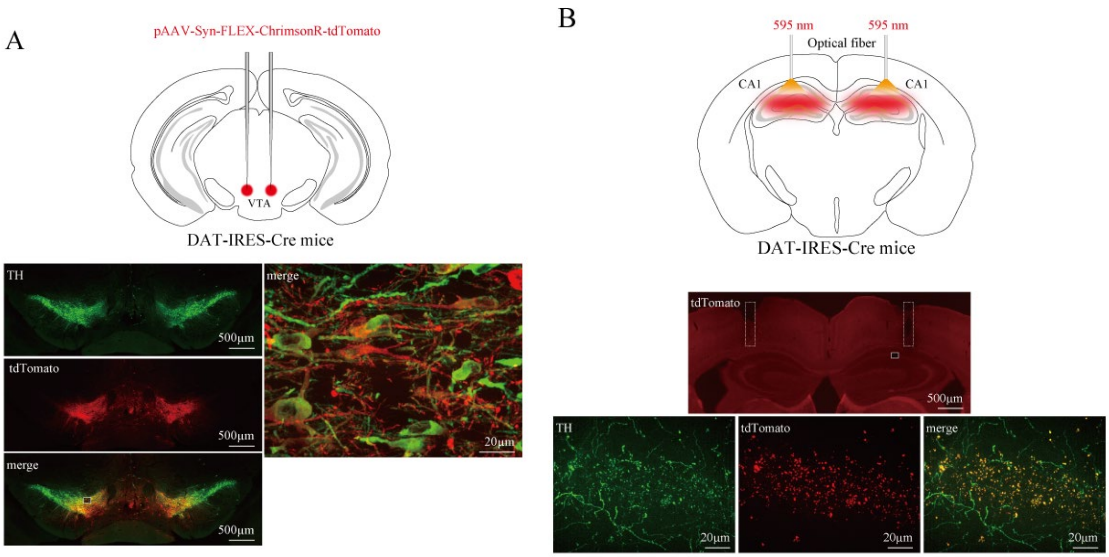

Figure 16. Schematic representation of the experimental setup for optogenetic stimulation to the dorsal hippocampal CA1 of DAT^{VTA} mice.

(A) Injection of pAAV-Syn-FLEX-ChrimsonR-tdTomato into the VTA of DAT-IRES-Cre mice generated DAT^{VTA} mice (top, left). Representative injection sites in tyrosine hydroxylase (TH)-stained coronal sections of DAT^{VTA} mice (bottom, left). The co-stained regions (yellow) indicate an overlap between AAV infection (red) and TH-stained areas (green), primarily localized to the VTA. The area within the white rectangle is presented in a magnified view. (B) We proceed with the bilateral insertion of an optical fiber for optogenetic stimulation into the dorsal hippocampal CA1 of DAT^{VTA} mice (top, right). Representative insertion sites in coronal sections of DAT^{VTA} mice (middle, right). The dashed rectangle depicts the tip of the optical fiber. The area within the white rectangle is presented in a magnified view (bottom, right). The co-stained regions (yellow) indicate an overlap between tdTomato expression (red) and TH-stained areas (green).

This figure is adapted from Tamatsu et al. 2023.

We applied two types of burst photo stimulation for 1 s with a long (40 ms) or short (10 ms) duration and 20-Hz pulse pattern during the changing reward location task at three different times: pre-stim, that is, after the infrared-blocking sensor situated 15 cm in front of the reward location was passed; post-stim, that is, 1 s after nose-poking at the reward location; and opposite-stim, that is, after the infrared-blocking sensor situated 15 cm in front of the opposite side of the reward location (e.g., south when the reward location was north) was passed (Figure 17).

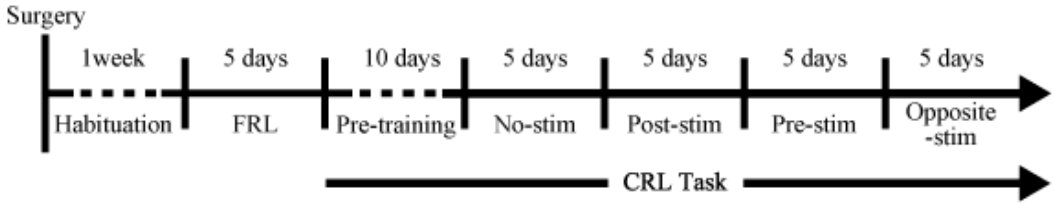

Figure 17. Experimental timeline.

Experimental timeline illustrating the sequence of behavioral tasks and optogenetic stimulation. Mice undergo 1 week of habituation to the maze, followed by 5 days of training in the fixed reward location (FRL) task. Subsequently, mice receive 10 days of pre-training in the changing reward location (CRL) task and then perform the CRL task with various stimulation conditions (no-stim, post-stim, pre-stim, and opposite-stim) for 5 days.

This figure is adapted from Tamatsu et al. 2023.

Short burst stimulation at pre-stim and post-stim did not significantly affect either the correct response rate or rule learning rate (Figure 18A-B; pre-stim: correct response: $F_{1,4}$

= 7.10, $P > 0.05$, rule learning: $F_{1,4} = 7.17$, $P > 0.05$; post-stim: correct response: $F_{1,4} = 5.51$, $P > 0.05$, rule learning: $F_{1,4} = 5.51$, $P > 0.05$, two-way repeated-measures ANOVA, n = 5 mice).

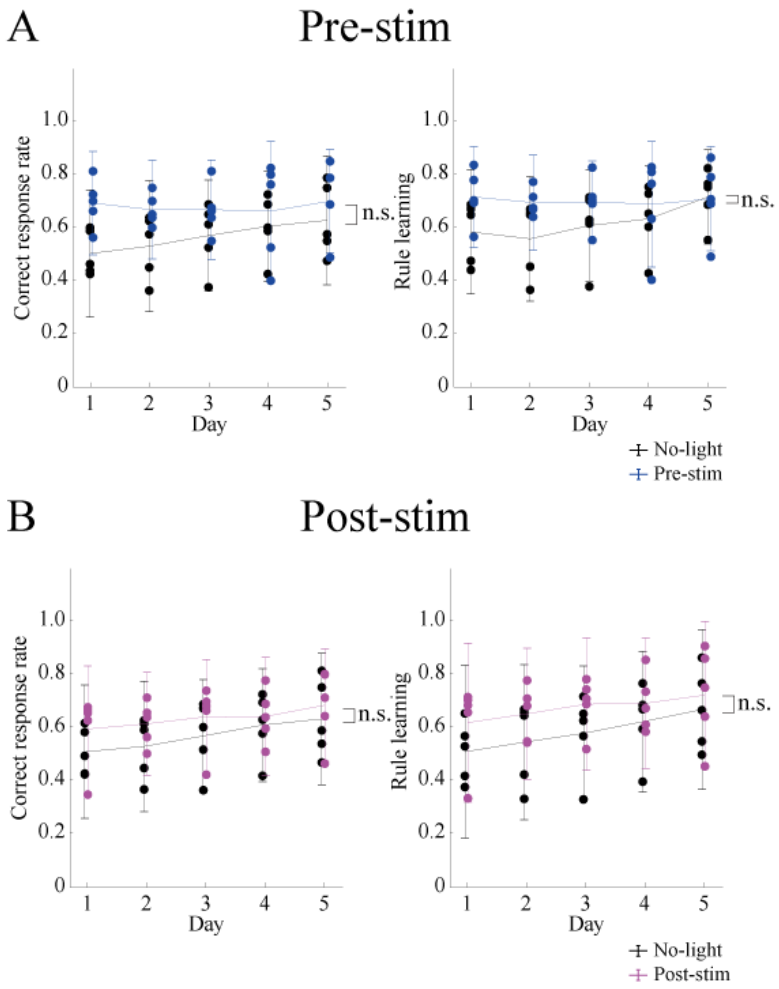

Figure 18. Short-duration burst stimulation does not significantly affect correct response rates or rule learning.

(A-B) Correct response rate (left) and rule learning rate (right) for the changing reward location task with short-duration burst stimulation at the pre-stim (A) or post-stim (B) conditions. Dots represent raw data points for individual mice, while the graph displays the mean ± standard deviation (SD). Statistical significance is determined using two-way mixed ANOVA. n.s.: $P > 0.05$.

This figure is adapted from Tamatsu et al. 2023.

In contrast, long burst stimulation at pre-stim and post-stim led to learning of the fast adaptation to the changed reward location from the first day, and there were significant differences in both the correct response and rule learning rates compared with those of the control group (Figure 19A-B; pre-stim: correct response: $F_{1,5} = 9.97$, $P < 0.05$, interaction: $P > 0.05$, rule learning: $F_{1,5} = 17.4$, $P < 0.01$, interaction: $P > 0.05$, Greenhouse–Geisser-corrected; post-stim: correct response: $F_{1,5} = 19.0$, $P < 0.01$, interaction: $P > 0.05$, rule learning: $F_{1,5} = 22.4$, $P < 0.01$, interaction: $P > 0.05$, Greenhouse–Geisser corrected, two-way repeated-measures ANOVA, n = 6 mice).

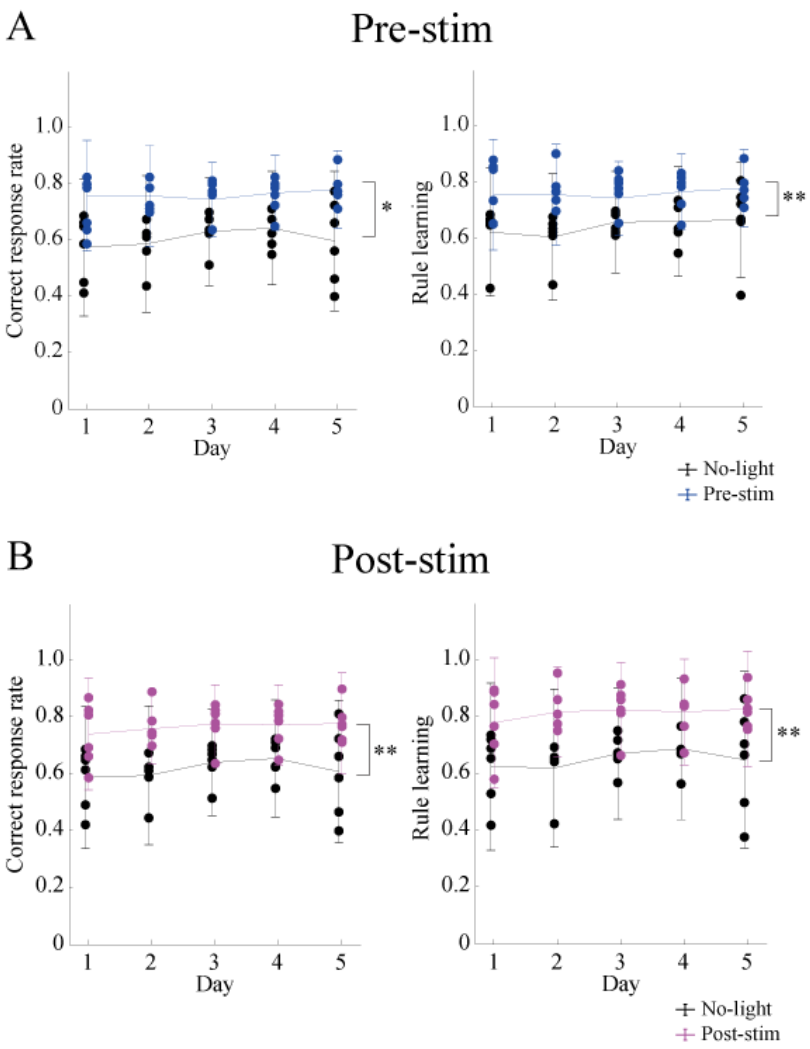

Figure 19. Long-duration burst stimulation significantly affects correct response rates or rule learning.

(A-B) Correct response rate (left) and rule learning rate (right) for the changing reward location task with long-duration burst stimulation at the pre-stim (A) or post-stim (B) conditions. Dots represent raw data points for individual mice, while the graph displays the mean ± standard deviation (SD). Statistical significance is determined using two-way mixed ANOVA. *: $P < 0.05$, **: $P < 0.01$.

This figure is adapted from Tamatsu et al. 2023.

This timing-invariant effect implies that this involvement is independent of internal events around the reward location, such as hippocampal reward cells or place cell activity. Furthermore, there was no significant difference in running speed toward the reward location between the short- and long-duration burst stimulations, regardless of whether the conditions were pre-stim or post-stim (Figure 20A-B; pre-stim: $F_{1,7} = 0.0251$, $p > 0.05$; post-stim: $F_{1,9} = 0.781$, $P > 0.05$; two-way mixed ANOVA). These findings show that the rapid goal adaptation effect is not solely attributed to heightened motivation or motor activity around the reward location caused by long-duration burst stimulation of the VTA-hippocampal dopaminergic pathway.

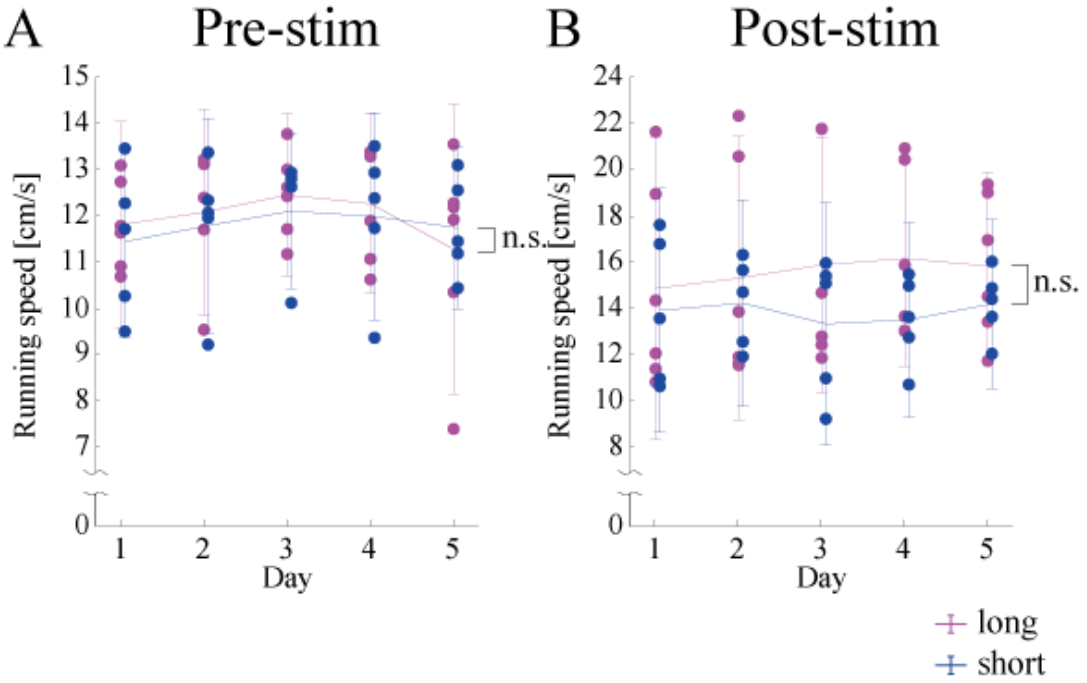

Figure 20. Motor performance does not change with the intensity of stimulation.
(A-B) The running speed to reach the reward location during the changing reward location task performance at the pre-stim (A) or post-stim (B) conditions. Dots represent raw data points for individual mice, while the graph displays the mean ± standard deviation (SD). Statistical significance is determined using two-way mixed ANOVA. n.s.: $P > 0.05$.
This figure is adapted from Tamatsu et al. 2023.

One well-established role of VTA dopaminergic neurons is to encode reward prediction errors. Interestingly, the long-duration burst stimulation of opposite-stim also led to significant outperformance in the changing reward location task (opposite-stim: correct response: $F_{1,5} = 8.76$, $P < 0.05$, interaction: $P > 0.05$; rule learning: $F_{1,5} = 7.88$, $P < 0.05$, interaction: $P > 0.05$, Greenhouse–Geisser-corrected, two-way repeated-measures

ANOVA, n = 6 mice; Figure 21). This location-invariant effect shows that the enhancement is independent of the reward prediction signals but solely dependent on the activation of VTA dopaminergic inputs.

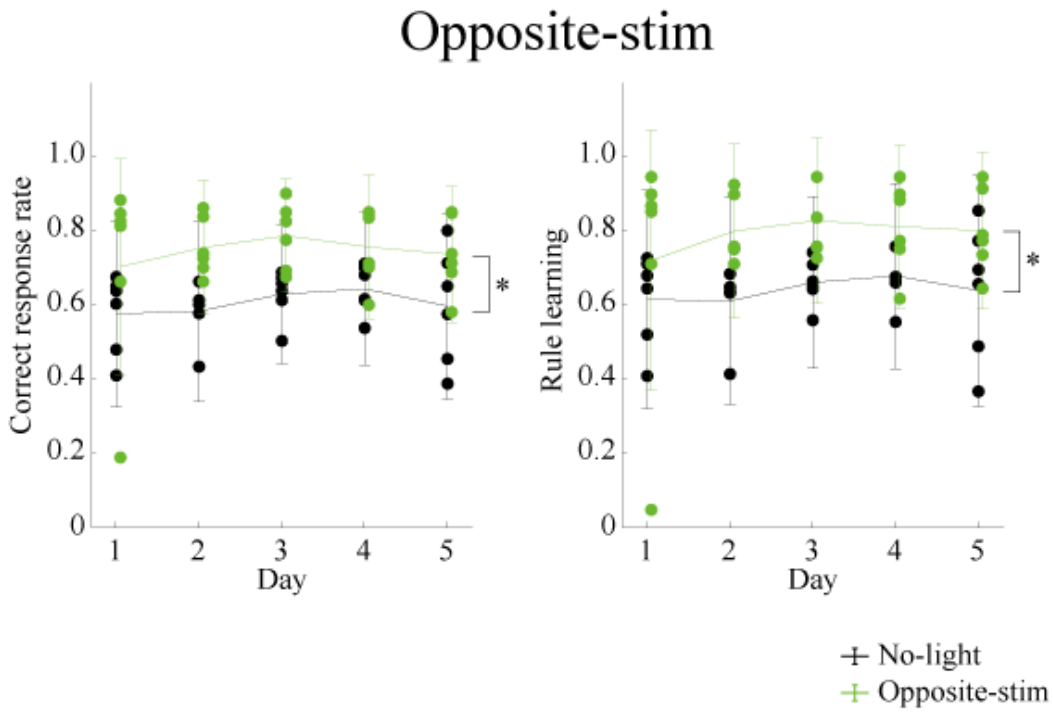

Figure 21. Long-duration burst stimulation of opposite-stim also improved task performance.

Correct response rate (left) and rule learning rate (right) for the changing reward location task with long-duration burst stimulation at the opposite-stim condition. Dots represent raw data points for individual mice, while the graph displays the mean ± standard deviation (SD). Statistical significance is determined using two-way mixed ANOVA. *: $P < 0.05$.

This figure is adapted from Tamatsu et al. 2023.

4.5 Distinct hippocampal responses to burst stimulation in the VTA-hippocampal pathway

Finally, to isolate the impact of stimulation duration on hippocampal activity, we examined how axonal excitation of VTA dopaminergic neurons influenced the activity of hippocampal CA1 pyramidal cells of freely roaming DAT^{VTA} mice in an open field using fiber photometry, thereby eliminating task-related confounds. An adeno-associated virus (AAV) vector containing a CaMKIIα promoter construct encoding GCaMP6f was injected into the pyramidal cells of the dorsal hippocampal CA1 (Figure 22).

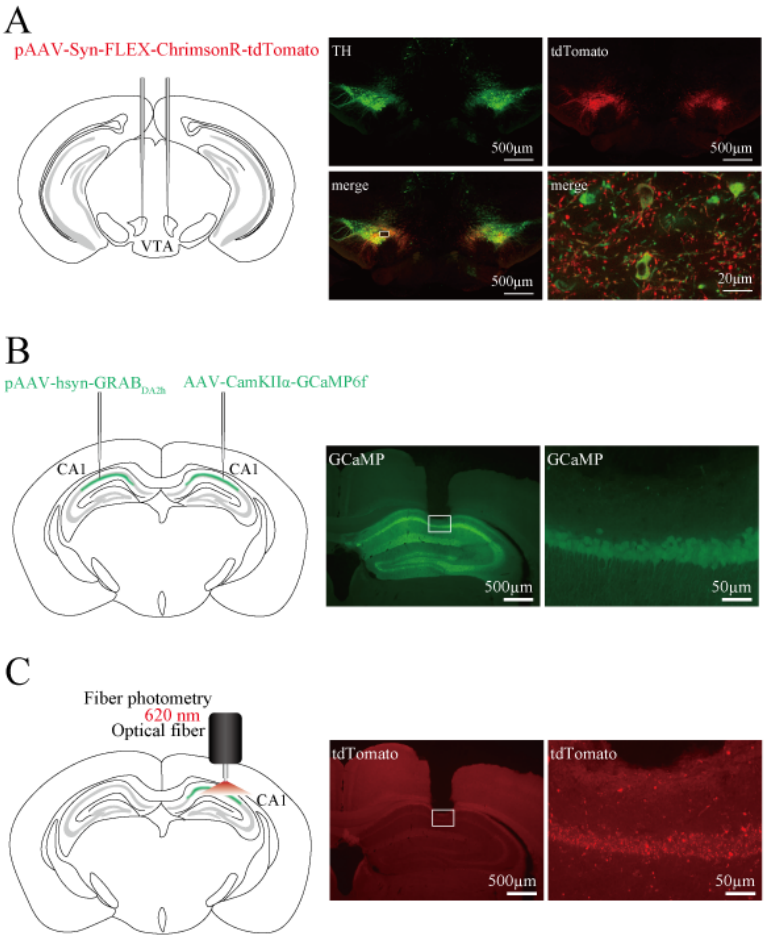

Figure 22. Schematic representation of the experimental setup for concurrent optogenetic and fiber photometry investigation.

(A) Bilateral injection of pAAV-Syn-FLEX-ChrimsonR-tdTomato into the VTA of DAT-IRES-Cre mice generated DAT^{VTA} mice (left). Representative injection sites in TH-stained coronal sections of DAT^{VTA} mice (right). The co-stained regions (yellow) indicate an overlap between tdTomato expression (red) and TH-stained areas (green), primarily localized to the VTA. The area within the white rectangle is presented in a magnified view. (B) Unilateral injection of AAV-CamKIIα-GCaMP6f and/or pAAV-hsyn-GRAB$_{DA2h}$ into the dorsal hippocampus of the DAT^{VTA} mice was performed (left). Representative GCaMP6f expression in the coronal section of the dorsal hippocampus of the DAT^{VTA} mice (right). (C) Calcium or dopamine signals are recorded via unilateral insertion of an optical fiber into the dorsal hippocampal CA1 of the DAT^{VTA} mice while simultaneously stimulating the VTA dopaminergic axons (left). Representative tdTomato expression in the coronal section of the dorsal hippocampus of DAT^{VTA} mice (right).

This figure is adapted from Tamatsu et al. 2023.

The excitation level during the long-duration burst pattern was consistently higher throughout the entire 180-second stimulation period than the 1-second pre-stimulation level. In contrast, the short-duration burst pattern, commonly employed in previous studies(McNamara et al. 2014; Tsetsenis et al. 2021), produced a less stable effect. There was a significantly higher count of responses exceeding the predetermined threshold level for long-duration burst stimulations than for short-duration stimulations ($P < 0.001$, Wilcoxon signed-rank test, n = 14 mice; Figure 23).

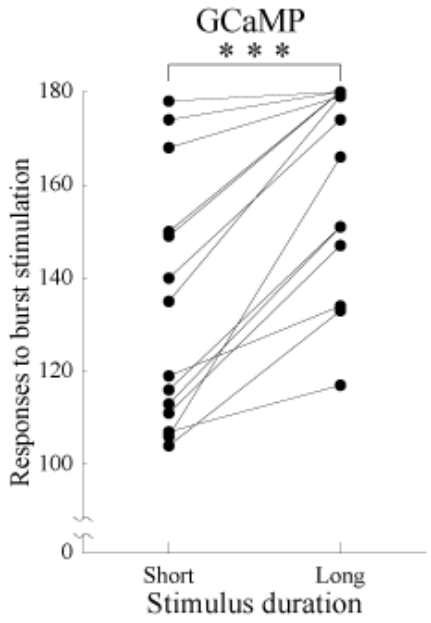

Figure 23. Long-duration burst stimulation activates neuronal activity in the dorsal hippocampus more effectively.

The count of GCaMP6f responses to burst stimulations that exceed the predetermined threshold level as a function of the duration of stimulation. Wilcoxon signed-rank test, ***: $P < 0.001$, GCaMP6f: n = 14 mice.

This figure is adapted from Tamatsu et al. 2023.

To analyze the corresponding behavioral outputs, the behavior was categorized into three groups based on their velocities: ambulation, immobility, and fine movement. There were no significant differences in the distribution of these behavioral periods ($P > 0.05$, multiple Wilcoxon signed-rank test with Bonferroni correction, n = 9 mice; Figure 24).

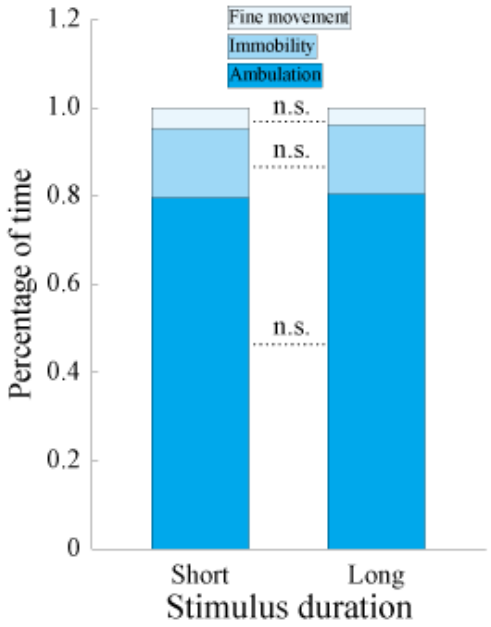

Figure 24. Behavioral performance is not affected by the stimulation.

Percentage of time of motor behavioral events (ambulation, immobility, and fine movement) as a function of the duration of stimulation (short or long). Multiple Wilcoxon signed-rank test with Bonferroni correction, n.s.: $P > 0.05$. n = 9 mice.

This figure is adapted from Tamatsu et al. 2023.

Most events involved ambulation; thus, we further analyzed the duration of ambulation and the findings showed that the long-duration burst pattern extended ambulation duration ($P < 0.05$, Wilcoxon signed-rank test, n = 9 mice; Figure 25).

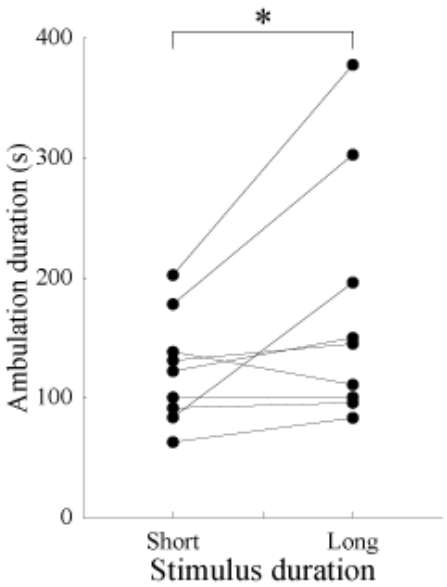

Figure 25. Long-duration burst pattern extends ambulation duration.

The graphs illustrate the ambulation duration as a function of the duration of stimulation. Wilcoxon signed-rank test, *: $P < 0.05$, n = 9 mice.

This figure is adapted from Tamatsu et al. 2023.

For calcium signaling in response to short- and long-duration burst stimulations (Figure 26A-B), there were significant differences across all examined time windows (during stimulation: $P < 0.001$; 2-5 s post-stimulation: $P < 0.01$; 5-8 s post-stimulation: $P < 0.001$; Wilcoxon signed-rank test, n = 14 mice, Figure 26C-D).

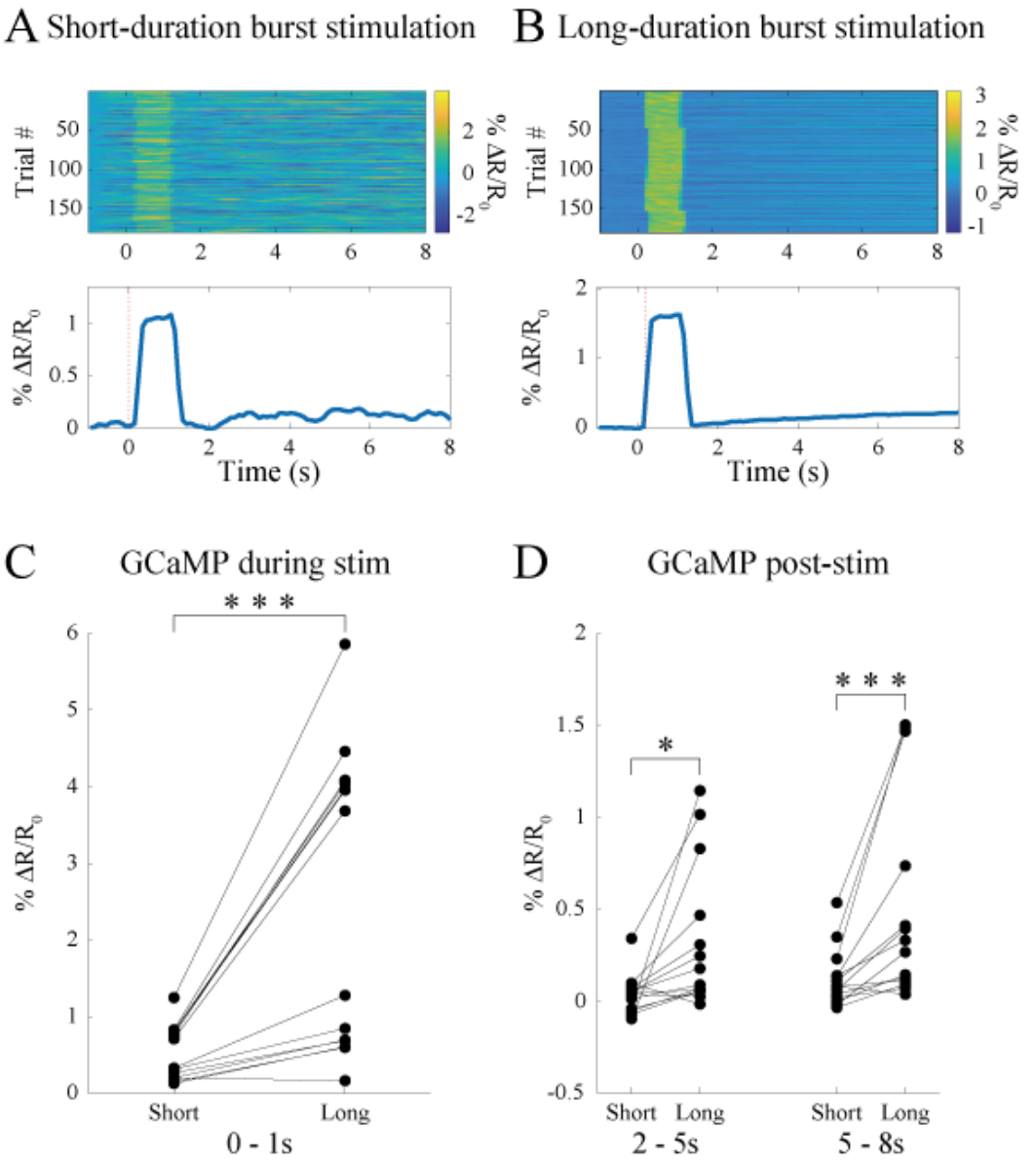

Figure 26. Long-duration burst stimulation patterns activate calcium signaling more effectively.

(A-B) Representative % ΔR / R_0 calcium signals from a mouse during individual trials (top) and averaged across trials (bottom) during short (A) and long (B) burst stimulations. Individual signal intensity is color-coded, as detailed in the color bar on the right. (C-D) Average % ΔR / R_0 calcium signals during stimulation (0–1s) (C) or early (2–5s) or late (5–8s) phase of post-stimulation (D) as a function of the duration of stimulation (short or long) (n = 14 mice).

This figure is adapted from Tamatsu et al. 2023.

To specifically gauge dopaminergic activity, we used an AAV vector encoding the $GRAB_{DA2h}$ sensor under a human synapsin promoter and targeted the dorsal hippocampal CA1. Unlike the pyramidal cell activity, the excitation level of dopamine responses during the short- and long-duration burst pattern was consistently higher throughout the entire 180-s stimulation period than those in the 1-s pre-stimulation period. Responses exceeding the predetermined threshold for long-duration burst stimulations were not significantly higher than that for short-duration stimulations ($P > 0.05$, Wilcoxon signed-rank test, n = 11 mice; Figure 27).

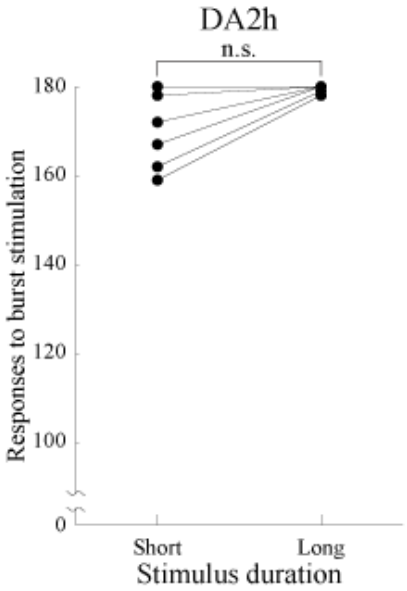

Figure 27. Dopamine activity shows no significant difference with stimulation.

The count of $GRAB_{DA2h}$ responses to burst stimulations that exceed the predetermined threshold level as a function of the duration of stimulation. Wilcoxon signed-rank test, n.s.: $P > 0.05$, $GRAB_{DA2h}$: n = 11 mice.

This figure is adapted from Tamatsu et al. 2023.

For dopaminergic signals elicited by short- and long-duration bursts (Figure 28A-B), there were significant differences during stimulation ($P < 0.001$, Wilcoxon signed-rank test) but not after stimulation (2–5s and 5–8s post-stimulation: $P > 0.05$; Wilcoxon signed-rank test) (n = 11 mice, Figure 28C-D).

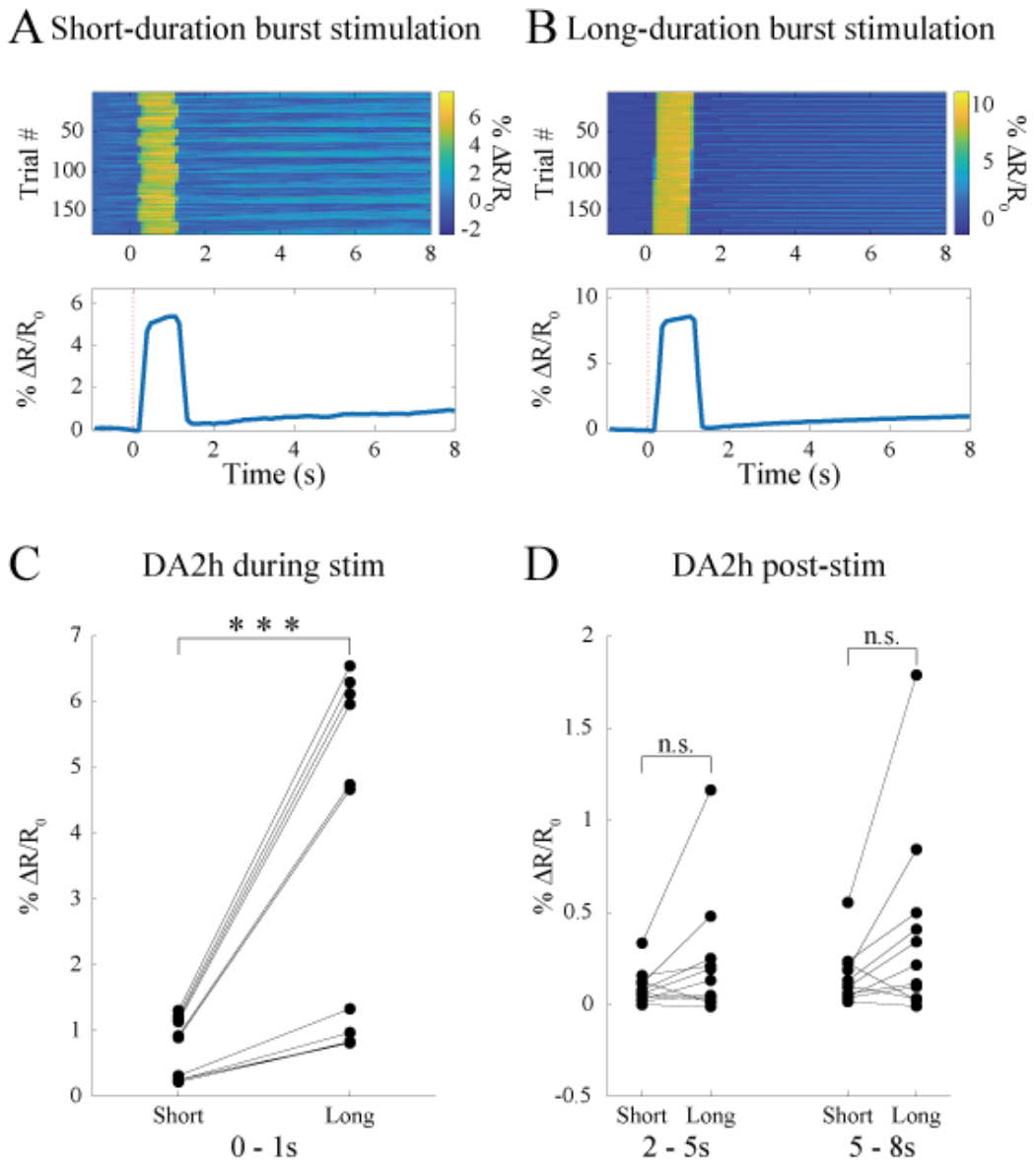

Figure 28. During stimulation, long-duration burst stimulation results in stronger dopamine activity.

(A-B) Representative % ΔR / R_0 dopaminergic responses from a mouse during individual trials (top) and averaged across trials (bottom) during short (A) and long (B) burst stimulations. Individual signal intensity is color-coded, as detailed in the color bar on the right. (C-D) Average % ΔR / R_0 dopaminergic responses during stimulation (0–1s) (C) or early (2–5s) or late (5–8s) phase of post-stimulation (D) as a function of the duration of stimulation (short or long) (n = 11 mice). Wilcoxon signed-rank test, *: $P < 0.05$, ***: $P < 0.001$, n.s.: $P > 0.05$.

This figure is adapted from Tamatsu et al. 2023.

Chapter 5. Discussion

5.1 Deficiency in VTA Dopamine Neurons Suppresses Memory of Reward Location

The hippocampus plays a crucial role in forming cognitive maps, particularly in the context of spatial navigation, as supported by the identification of essential place cells for determining goal locations (Mamad et al. 2017; Pfeiffer and Foster 2013; Sarel et al. 2017). The midbrain limbic dopamine system is a key modulator in various learning processes. Recent evidence suggests that studies on reward cells in the hippocampus indicate that dopamine input from the VTA to the hippocampus contributes to the persistence and adaptation of reward-related cognitive maps (Gauthier and Tank 2018; McNamara et al. 2014). However, the causal relationship between dopamine input to the hippocampus and rapid adaptation to these goals is yet to be fully elucidated.

Our study demonstrated that a deficiency in VTA dopamine neurons significantly impairs the ability to reliably remember reward locations. This is consistent with previous studies on the effects of VTA dopamine axons in the hippocampus (Kempadoo et al. 2016; McNamara et al. 2014; Takeuchi et al. 2016). Since VTA dopamine neurons are deeply involved in reward processing, their deficiency is thought to inhibit the consolidation of memory for reward locations. However, during the deficiency of VTA dopamine neurons,

some SNc dopamine neurons were also lost. The loss of SNc dopamine neurons, a cause of Parkinson's disease, has led to significant motor impairments. Considering that both the reduction in motivation due to the loss of VTA dopamine neurons and motor impairments from the loss of SNc dopamine neurons could affect spatial memory, we believed experiments that suppress or deplete dopamine within the hippocampus are necessary.

5.2 Inhibition of Dopamine Receptors in the Hippocampus Suppresses Movement

When we pharmacologically inhibited the dopamine receptors in the dorsal hippocampus, we observed more severe impairments in movement and motivation than in lesion experiments. Although we used a method similar to the one in Morris's experiment, such severe motor impairments have not been reported. This could be due to the environmental differences in our study, where mice were confined to a maze at a higher position, while the prior studies allowed free movement in an open field. Unfortunately, this difference in motor performance cannot be clearly determined from our experiment.

Apart from the VTA dopamine input, the hippocampus also receives dopamine input from the locus coeruleus (LC). It is known that LC dopamine input is involved in spatial

learning for remembering reward locations. Since our study inhibited the effects of dopamine from both dopaminergic pathways projecting to the hippocampus, it suggested that the impairments in movement and motivation are not solely due to the midbrain limbic VTA dopamine pathway, independent of the hippocampus. Therefore, targeting the VTA dopamine input to the hippocampus is a critical element in understanding the relationship between dopamine signaling in the hippocampus and dynamic adaptation to goal locations.

5.3 Activation of VTA Dopamine Neurons in the Hippocampus is Related to Rapid Adaptation to Goal Locations

Our observations on rapid adaptation to goal locations can be analyzed through the lens of four different hypotheses. The Timing Hypothesis emphasizes that the timing of neural excitation, especially in conjunction with receiving rewards, is a critical determinant in optimizing cognitive performance (Glimcher 2011). The Training Hypothesis proposes that repetitive patterns of neural excitation function as a form of neural 'conditioning,' helping to overcome barriers in translating learned knowledge into action (Covey and Cheer 2019; Kesner, Calva, and Ikemoto 2022). The Threshold Hypothesis suggests that a certain degree or threshold of neural excitation is a prerequisite for cognitive enhancement (Coddington, Lindo, and Dudman 2023). Finally, the Specificity

Hypothesis argues that a subset of neurons or their connections within the VTA-hippocampus dopamine pathway are crucial for cognitive improvement (Ioanas, Saab, and Rudin 2022; J. E. Lisman and Grace 2005).

5.3.1 Timing Hypothesis

We observed that when optogenetic stimulation accurately targets the dorsal hippocampus with VTA dopamine inputs, adaptation to changes in reward locations becomes more rapid. This rapid adaptation was evident in the consistency and specificity of goal adaptation, unlike with non-stimulated inputs. Our findings challenge the notion that artificial stimulation near food dispensers coincidentally induces cessation of movement and rapid change of reward locations. Notably, even when the same stimulation was applied under so-called counter-stimulus conditions at locations not normally associated with reward locations, a significant improvement in goal adaptation was observed. Furthermore, prolonged burst stimulation of the VTA-hippocampus dopamine pathway seemed to promote walking. These observations suggest that activation operates independently of reward-related processes such as reward prediction error signals. Therefore, the importance of the timing of neural excitation as presented in the Timing Hypothesis might not be as critical as previously thought, although it may still contribute to overall cognitive performance in more subtle ways.

5.3.2 Training Hypothesis

Interestingly, the rapid response to changes in goal locations showed a significant improvement in performance compared to non-stimulated conditions. This observation suggests that dopamine input from the VTA may function as an 'instructive signal' in the hippocampus, enhancing cognitive performance as proposed by the Training Hypothesis. However, this hypothesis does not fully explain the improvements observed under counter-stimulus conditions. This finding indicates that, although mice appear to quickly learn the changes in updated goal locations, they may encounter resistance when attempting to translate this learned knowledge into action. Dopamine input from the VTA is thought to alleviate this resistance, facilitating the expression of learned behaviors. Future research should explore the potential factors contributing to this resistance, especially synaptic plasticity, neuromodulation, and various intracellular signaling pathways (Tsetsenis, Broussard, and Dani 2023).

5.3.3 Threshold Hypothesis

The current study explores the role of VTA dopamine input in the dorsal hippocampus, presenting a contrasting perspective to previous research that examined the persistence and reactivation of spatial memory (McNamara et al. 2014). Our results have revealed that the short-duration burst optogenetic stimulation used in previous studies was

insufficient to drive rapid goal adaptation. A critical aspect of this discrepancy stems from the differences in both the intensity and type of optogenetic tools used. While the earlier study used laser-based optogenetic stimulation with an intensity ranging from 10-20 mW to activate ChR2 (McNamara et al. 2014), our approach involved a significantly lower intensity of only 2.5 mW using LED to activate ChrimsonR. This supports the idea, as proposed by the Threshold Hypothesis, that the VTA-hippocampus dopamine pathway exhibits multifaceted functions regulated by specific activation patterns and/or intensities.

5.3.4 Specificity Hypothesis

The observed improvement in spatial goal adaptation cannot be attributed solely to the release of dopamine. This may also involve the co-release of neurotransmitters such as glutamate and gamma-aminobutyric acid (GABA) (Stuber et al. 2010; Tritsch et al. 2014). This assertion is supported by the significant increase in the excitability of hippocampal pyramidal cells during prolonged burst stimulation of VTA-derived axons, which persists even after the stimulation, unlike more transient dopamine signals. This suggests that not only dopamine but also the co-released glutamate and/or GABA may contribute to enhanced spatial goal adaptation.

5.4 Summary

In summary, our research provides valuable insights into the role of dopamine input in the dorsal hippocampus in facilitating rapid adaptation to goal locations during spatial navigation. However, further research is necessary for a more comprehensive understanding of the involved neural mechanisms. This includes investigating the contribution of other neurotransmitter systems, the potential role of remapping place fields, and exploring the specific functions of distinct activation patterns within the VTA-hippocampus dopamine pathway. Addressing these limitations and building upon our current findings, we can advance our knowledge of the neural underpinnings of goal-directed navigation and cognitive map formation.

Chapter 6. Future Perspectives

Previous studies have demonstrated the relationship between the formation of goal-related cognitive maps in the hippocampus and local dopamine release using dopamine receptor blockers and electrophysiological methods. According to this research, when reward locations are changed without dopamine, remapping of place fields is suppressed. Based on this concept, exciting axons of VTA dopamine neurons in the hippocampus may promote the induction of remapping of place fields. Conversely, as seen in previous studies on reward cells, place cells may not undergo remapping of place fields. Instead, only the place fields of reward cells might shift rapidly. While our methodology cannot answer these questions, the results emphasize the importance of exciting VTA dopamine neurons in the hippocampus in adapting to changes in reward locations during goal-directed navigation.

Future research could compare the results of stimulating axons of other projection targets of VTA dopamine neurons. Additionally, applying cell-type-specific inhibition of VTA dopamine neuron activity could elucidate the contribution of each projection site, provide a comprehensive understanding of the underlying neural mechanisms, and support the specificity hypothesis.

References

Bruno, Carissa A. et al. 2020. “pMAT: An Open-Source, Modular Software Suite for the Analysis of Fiber Photometry Calcium Imaging.” : 2020.08.23.263673. https://www.biorxiv.org/content/10.1101/2020.08.23.263673v1 (April 28, 2023).

Coddington, Luke T., Sarah E. Lindo, and Joshua T. Dudman. 2023. “Mesolimbic Dopamine Adapts the Rate of Learning from Action.” *Nature* 614(7947): 294–302.

Cohen, Jeremiah Y. et al. 2012. “Neuron-Type Specific Signals for Reward and Punishment in the Ventral Tegmental Area.” *Nature* 482(7383): 85–88.

Covey, Dan P., and Joseph F. Cheer. 2019. “Accumbal Dopamine Release Tracks the Expectation of Dopamine Neuron-Mediated Reinforcement.” *Cell Reports* 27(2): 481-490.e3.

Gauthier, Jeffrey L., and David W. Tank. 2018. “A Dedicated Population for Reward Coding in the Hippocampus.” *Neuron* 99(1): 179-193.e7.

Glimcher, Paul W. 2011. “Understanding Dopamine and Reinforcement Learning: The Dopamine Reward Prediction Error Hypothesis.” *Proceedings of the National Academy of Sciences* 108(supplement_3): 15647–54.

Hoshino, Satoshi et al. 2020. “The Reconfigurable Maze Provides Flexible, Scalable, Reproducible, and Repeatable Tests.” *iScience* 23(1): 100787.

Ioanas, Horea-Ioan, Bechara John Saab, and Markus Rudin. 2022. “Whole-Brain Opto-fMRI Map of Mouse VTA Dopaminergic Activation Reflects Structural Projections with Small but Significant Deviations.” *Translational Psychiatry* 12(1): 1–10.

Jain, Deepa, Indraja R. Jakhalekar, and Sachin S. Deshmukh. 2017. “Navigational Strategies and Their Neural Correlates.” *Journal of the Indian Institute of Science* 97(4): 511–25.

Kempadoo, Kimberly A. et al. 2016. “Dopamine Release from the Locus Coeruleus to the Dorsal Hippocampus Promotes Spatial Learning and Memory.” *Proceedings of the National Academy of Sciences* 113(51): 14835–40.

Kesner, Andrew J., Coleman B. Calva, and Satoshi Ikemoto. 2022. “Seeking Motivation and Reward: Roles of Dopamine, Hippocampus, and Supramammillo-Septal Pathway.” *Progress in Neurobiology* 212: 102252.

Kramar, Cecilia P. et al. 2021. “The Late Consolidation of an Aversive Memory Is Promoted by VTA Dopamine Release in the Dorsal Hippocampus.” *European Journal of Neuroscience* 53(3): 841–51.

Kravitz, Alexxai V. et al. 2010. “Regulation of Parkinsonian Motor Behaviours by Optogenetic Control of Basal Ganglia Circuitry.” *Nature* 466(7306): 622–26.

Lerner, Talia N., Ashley L. Holloway, and Jillian L. Seiler. 2021. “Dopamine, Updated: Reward Prediction Error and Beyond.” *Current opinion in neurobiology* 67: 123–30.

Lisman, John et al. 2017. “Viewpoints: How the Hippocampus Contributes to Memory, Navigation and Cognition.” *Nature neuroscience* 20(11): 1434–47.

Lisman, John E., and Anthony A. Grace. 2005. “The Hippocampal-VTA Loop: Controlling the Entry of Information into Long-Term Memory.” *Neuron* 46(5): 703–13.

Mamad, Omar et al. 2017. “Place Field Assembly Distribution Encodes Preferred Locations.” *PLoS Biology* 15(9): e2002365.

Mathis, Alexander et al. 2018. “DeepLabCut: Markerless Pose Estimation of User-Defined Body Parts with Deep Learning.” *Nature Neuroscience* 21(9): 1281–89.

McNamara, Colin G. et al. 2014. “Dopaminergic Neurons Promote Hippocampal Reactivation and Spatial Memory Persistence.” *Nature Neuroscience* 17(12): 1658–60.

Naisbett-Jones, Lewis C., and Kenneth J. Lohmann. 2022. “Magnetoreception and Magnetic Navigation in Fishes: A Half Century of Discovery.” *Journal of Comparative Physiology A* 208(1): 19–40.

O'Carroll, Colin M. et al. 2006. "Dopaminergic Modulation of the Persistence of One-Trial Hippocampus-Dependent Memory." *Learning & Memory* 13(6): 760–69.

O'Keefe, J., and J. Dostrovsky. 1971. "The Hippocampus as a Spatial Map. Preliminary Evidence from Unit Activity in the Freely-Moving Rat." *Brain Research* 34(1): 171–75.

Pfeiffer, Brad E., and David J. Foster. 2013. "Hippocampal Place-Cell Sequences Depict Future Paths to Remembered Goals." *Nature* 497(7447): 74–79.

Retailleau, Aude, and Genela Morris. 2018. "Spatial Rule Learning and Corresponding CA1 Place Cell Reorientation Depend on Local Dopamine Release." *Current Biology* 28(6): 836–46.

Sarel, Ayelet, Arseny Finkelstein, Liora Las, and Nachum Ulanovsky. 2017. "Vectorial Representation of Spatial Goals in the Hippocampus of Bats." *Science (New York, N.Y.)* 355(6321): 176–80.

Sawatani, Fumiya et al. 2022. "Utilizing a Reconfigurable Maze System to Enhance the Reproducibility of Spatial Navigation Tests in Rodents." *Journal of Visualized Experiments: JoVE* (190).

Schultz, W., P. Dayan, and P. R. Montague. 1997. "A Neural Substrate of Prediction and Reward." *Science (New York, N.Y.)* 275(5306): 1593–99.

Stuber, Garret D. et al. 2010. "Dopaminergic Terminals in the Nucleus Accumbens But Not the Dorsal Striatum Corelease Glutamate." *The Journal of Neuroscience* 30(24): 8229–33.

Takeuchi, Tomonori et al. 2016. "Locus Coeruleus and Dopaminergic Consolidation of Everyday Memory." *Nature* 537(7620): 357–62.

Tamatsu, Yuta et al. 2023. "Optogenetic Activation of the Ventral Tegmental Area-Hippocampal Pathway Facilitates Rapid Adaptation to Changes in Spatial Goals." *iScience* 26(12). https://www.cell.com/iscience/abstract/S2589-0042(23)02613-5 (December 4, 2023).

Tolman, Edward C. 1948. “Cognitive Maps in Rats and Men.” *Psychological Review* 55(4): 189–208.

Tritsch, Nicolas X, Won-Jong Oh, Chenghua Gu, and Bernardo L Sabatini. 2014. “Midbrain Dopamine Neurons Sustain Inhibitory Transmission Using Plasma Membrane Uptake of GABA, Not Synthesis” ed. Gary L Westbrook. *eLife* 3: e01936.

Tsetsenis, Theodoros et al. 2021. “Midbrain Dopaminergic Innervation of the Hippocampus Is Sufficient to Modulate Formation of Aversive Memories.” *Proceedings of the National Academy of Sciences* 118(40): e2111069118.

Tsetsenis, Theodoros, John I. Broussard, and John A. Dani. 2023. “Dopaminergic Regulation of Hippocampal Plasticity, Learning, and Memory.” *Frontiers in Behavioral Neuroscience* 16: 1092420.

Yamada, Yasufumi et al. 2020. “Modulation of Acoustic Navigation Behaviour by Spatial Learning in the Echolocating Bat Rhinolophus Ferrumequinum Nippon.” *Scientific Reports* 10(1): 10751.

Zhuang, Xiaoxi et al. 2005. “Targeted Gene Expression in Dopamine and Serotonin Neurons of the Mouse Brain.” *Journal of Neuroscience Methods* 143(1): 27–32.